

POWER SYSTEM STABILIZER DESIGN

USING

PARTICLE SWARM OPTIMIZATION

Thesis submitted in the partial fulfilment of requirement for the award of the Degree of

MASTER OF ENGINEERING

IN

POWER SYSTEMS AND ELECTRIC DRIVES

Submitted by

Sameer Bhambri

Roll. No. 800841014

Under guidance of

Mr. Nitin Narang

Assistant Professor, EIED



ELECTRICAL AND INSTRUMENTATION ENGINEERING DEPARTMENT

THAPAR UNIVERSITY

PATIALA-147004

JULY-2010

CERTIFICATE

I hereby certify that the work which is being presented in this thesis entitled, "*Power System Stabilizer Design Using Particle Swarm Optimization Algorithm*" in the partial fulfilment of the requirements for the award of the degree of Master of Engineering in "*Power Systems and Electric Drives*" Submitted in Electrical and Instrumentation Engineering Department of Thapar University, Patiala is an authentic record of my own work carried out under the supervision of Mr Nitin Narang (Assistant Professor, EIED)

The matter presented in this thesis has not been submitted any where for the award of any other degree.


(Sameer Bhambri)

Roll no 800841014

This is to certify that above statement made by candidate is correct and true to the best of my knowledge.



Mr Nitin Narang

Assistant Professor

Electrical and Instrumentation Engg Department

Thapar University, Patiala 147004

Countersigned by:


Dr. Smarajit Ghosh

Professor and Head, (EIED)

Thapar University

Patiala 147004


Dr. R.K Sharma

Dean (Acadmic Affairs)

Thapar University

Patiala 147004

ACKNOWLEDGEMENT

I would like to express my gratitude to my guide Mr. Nitin Narang, (Assistant Professor) Electrical and Instrumentation Engineering Department, Thapar University, Patiala for his patient guidance and support throughout this thesis work. I am truly very fortunate to have the opportunity to work with him. I found this guidance to be extremely valuable.

I am very thankful to the Head of the Department, Dr. Smarajit Ghosh, for his encouragement, support and providing the facilities for the completion of this thesis.

I am also thankful to entire faculty and staff members of Electrical and Instrumentation Engineering Department for their unyielding encouragement.

I would also like to acknowledge and express my deepest gratitude to my parents for their magnificent support and contributions to my journey and to the creation of this thesis.


Sameer Bhambri

800841014

ABSTRACT

Dynamic stability has challenged power system engineers since over three decades now. In the generator, the electromechanical coupling between the rotor and rest of the system causes oscillatory behaviour around the equilibrium state, following any disturbance. The use of fast acting high gain AVRs and evolution of large interconnected power systems with transfer of bulk power across weak transmission links have further aggravated the problem of low frequency oscillations. The oscillations, which are typically in the frequency range of 0.2 to 0.3 hertz, might be excited by the disturbances in the system or, in some cases, might even build up spontaneously. These oscillations limit the power transmission capability of a network and, sometimes, even cause a loss of synchronism and an eventual breakdown of the entire system.

The application of power system stabilizer can help in damping out these oscillations and improve the system stability. The traditional and till date the most popular solution to this problem is application of conventional power system stabilizer (CPSS). However, continual changes in the operating condition and network parameters result in corresponding change in system dynamics. This constantly changing nature of power system makes the design of CPSS a difficult task.

In this thesis work Particle Swarm Optimization algorithm has been used for tuning the parameters of a fixed gain power system stabilizer. The stabilizer places the troublesome system modes in an acceptable region in the complex plane and guarantees a robust performance over a wide range of operating conditions. Conventional lead/lag structure is retained but its parameters are retuned using Particle swarm optimization algorithm to obtain enhanced performance. Unlike GA and other heuristic algorithms, PSO has the flexibility to control the balance between the global and local exploration of the search space. This unique feature of PSO overcomes the premature convergence problem and enhances the search capability.

CONTENTS

CERTIFICATE

ACKNOWLEDGEMENT

ABSTRACT

i

LIST OF FIGURES

v

CHAPTER# 1

(1-09)

INTRODUCTION

1.1 Power System oscillations (Historical perspective) (1)

1.2 Low Frequency Oscillations (3)

1.3 Criteria for Damping (4)

1.4 Literature Review (5)

1.5 Scope of the Present Work (8)

1.6 Organization of the Thesis (9)

CHAPTER# 2

(10- 33)

SMALL SIGNAL STABILITY OF A SMIB SYSTEM

2.1 Introduction (10)

2.2 Synchronous machine model (11)

2.3 Classical model (11)

2.4 Variable voltage (E'_q) behind transient reactance (X'_d) model – no AVR (15)

2.5 Variable voltage ($E_{q'}$) behind transient reactance ($X_{d'}$) model – with exciter and AVR	(18)
2.6 Power System Stabilizer	(20)
2.7 Tuning Guidelines for the CPSS	(22)
2.8 Magnitude requirements	(27)
2.9 Operating Conditions	(28)
2.10 CPSS Parameter Selection	(28)
2.10.1 Eigenvalues	(28)
2.10.2 Damping	(28)
2.11 Simulation Study	(29)
2.10 Torque characteristics	(32)
CHAPTER#3	
PARTICLE SWARM OPTIMIZATION	(34- 43)
3.1 Introduction	(34)
3.2 Basic Particle Swarm Optimization	(35)
3.3 Flow Chart of Basic PSO	(38)
3.4 Test Example	(40)
3.5 Advantages	(43)
CHAPTER#4	(44- 48)
PROPOSED STABILIZATION TECHNIQUE	
SINGLE MACHINE SYSTEM	
4.1 Introduction	(44)

4.2 Objective Function	(45)
4.3 Algorithm	(46)
4.4 Flow Chart	(47)
CHAPTER#5	
RESULTS , CONCLUSION & FUTURE SCOPE	(49- 55)
5.1 Time Domain Simulation	(53-54)
5.2 Conclusion	(55)
APPENDIX A	(56)
APPENDIX B	(58)
REFERENCES	(60)

LIST OF FIGURES

Fig. 2.1 The equivalent circuit of synchronous machine connected to infinite bus system	(11)
Fig. 2.2 Classical model of generator	(12)
Fig. 2.3 Block diagram of single machine infinite bus system with classical model	(13)
Fig. 2.4 Block diagram representation with constant E_{fd}	(15)
Fig. 2.5 AVR BLOCK diagram representation with exciter and AVR	(19)
Fig. 2.6 Block diagram representation with AVR and PSS	(21)
Fig. 2.7 Thyristor excitation system with AVR and PSS	(22)
Fig. 2.8 Heffron- Phillips model of the SMIB System	(24)
Fig. 2.9 Magnitude and phase plot of transfer function GEP(s)	(25)
Fig. 2.10 Magnitude and phase plot of transfer function PSS(s)	(25)
Fig. 2.11 Magnitude and phase plot of transfer function GEP(s).PSS(s)	(26)
Fig. 2.12 Response of speed deviation without PSS (a) with CPSS (b) Load angle deviation without PSS (c) with CPSS (d) Terminal voltage deviation without PSS (e) with CPSS (f) PSS output (g)	(29-31)
Fig. 2.13 Torque characteristics	(32)
Fig. 3.1 The basic algorithm of PSO	(38)
Fig 3.2 Movement of an individual	(39)
Fig 3.3 The plot of global best solution (fitness) with iterations	(41)
Fig. 3.4 The plot of first dimension global best position with iterations	(41)
Fig. 3.5 The plot of second dimension global best position with iterations	(42)
Fig. 3.6 The plot of third dimension global best position with iterations	(42)

Fig. 4.1 The basic algorithm of PSO	(47)
Fig 5.1 Randomly initialized Eigen values in the complex plane	(50)
Fig 5.2 Shifted eigenvalues with respect to D- Contour	(51)
Fig 5.3 Eigen values corresponding to the local best parameters of the previous operating point	(52)
Fig 5.4 Shifted eigenvalues with respect to D- Contour	(53)
Fig 5.5 Response of speed deviation and Load angle deviation ($P = 0.9, Q = 0.1, X_e = 0.997$) (a), (b) ($P = 0.8, Q = 0.0, X_e = 0.897$) (c), (d)	(53-54)
Fig. B.1 D –contour in x – y plane	(58)

CHAPTER#1

INTRODUCTION

1.1 Power system oscillations

Historical perspective

Damping of oscillations in power system has been recognized as important in electric power system operations from the beginning. Before there were any power systems, oscillations in automatic speed controls (governors) initiated an analysis by J.C. Maxwell (speed controls were found necessary for the successful operation of the first steam engines). Apart from the immediate application of Maxwell's analysis, it also had a lasting influence as at least one of the stimulants to the development of very useful and widely used method by E. J. Routh in 1883, which enables one to determine theoretically the stability of a high order dynamic system without having to know the roots of its equations (Maxwell analyzed only a second order system).

Oscillations among generators appeared as soon as AC generators were operated in parallel. These oscillations were not unexpected, and in fact, were predicted from the concept of the power vs phase angle curve gradient interacting with the electric generator rotary inertia, forming an equivalent mass- and-spring system. With a continually varying load and some slight differences in the design and loading of the generators, oscillations tended to be continually excited. In the case of hydrogenerators, in particular, there was very little damping, and so amortisseurs (damper windings) were installed, at first as an option. (There was concern about the increased short-circuit current and some people had to be persuaded to accept them (Crary and Duncan, 1941).) It is of interest to note that although the only significant source of actual negative damping here was the turbine speed governor (Concordia, 1969), the practical "cure" was found elsewhere. Two points were evident then and are still valid today. First, automatic control is practically the only source of negative damping, and second, although it is obviously desirable to identify the sources of negative damping, the most effective and economical place to add damping may lie elsewhere.

After these experiences, oscillations seemed to disappear as a major problem. Although there were occasional cases of oscillations and evidently poor damping, the major analytical effort seemed to ignore damping entirely. First using analog and then digital, computing aids analysis of electric power system dynamic performance was extended to very large systems, but still representing the generators (and, for that matter, also the loads) in the simple “classical” way. Most studies covered only a short time-period, and as occasion demanded, longer-term simulations were kept in bound by including empirically estimated damping factors. It was, in effect, tacitly assumed that the net damping was positive.

All this changed rather suddenly in the 1960s, when the process of interconnection accelerated and more transmission and generation extended over large areas. Perhaps, the most important aspect was the wider recognition of the negative damping produced by the use of high-response generator voltage regulators in situations where the generator may be subject to relatively large angular swings, as may occur in extensive networks. (This possibility was already well known in the 1930s and 1940s but had not had much practical application then.) With the growth of extensive power systems, and especially with the interconnection of these systems by ties of limited capacity, oscillations reappeared [5,14].

1. For intersystem oscillations, the amortisseur is no longer effective, as the damping produced is reduced in approximately inverse proportion to the square of the effective external-impedance- plus-stator-impedance, and so it practically disappears.
2. The proliferation of automatic controls has increased the probability of adverse interactions among them. (Even without such interactions, the two basic controls—the speed governor and the generator voltage regulator—practically always produce negative damping for frequencies in the power system oscillation range: the governor effect, small and the AVR effect, large.)

Aside from this abbreviated account of how oscillations grew in importance as interconnections grew in extent, it may be of interest to mention the specific case that seemed to precipitate the general acceptance of the major importance of improving system damping, as well as the general recognition of the generator voltage regulator as the major culprit in producing negative damping. This was the series of studies of

the transient stability of the Pacific Intertie (AC and DC in parallel) on the west coast of the U.S. In these studies, it was noted that for three-phase faults, instability was determined not by severe first swings of the generators but by oscillatory instability of the post-fault system, which had one of two parallel AC line sections removed and thus higher impedance. This showed that damping is important for transient as well as steady-state conditions and contributed to a worldwide rush to apply *power system stabilizers (PSS)* to all generator-voltage regulators as a panacea for all oscillatory ills.

1.2 Low frequency oscillations

Electro-mechanical oscillations between interconnected synchronous generators are phenomena inherent to power systems. The stability of these oscillations is of vital concern, and is a prerequisite for secure system operation. For many years, the oscillations observed to be troublesome in power systems, were associated with a single generator, or a very closely connected group of units at a generating plant. Some low frequency unstable oscillations were also observed when large systems were connected by relatively weak tie lines, and special control methods were used to stabilize the interconnected system. These low frequency modes were found to involve groups of generators or plants, on one side of the tie oscillating against groups of generators on the other side of the tie.

In a generator, the electro-mechanical coupling between rotor and rest of the system causes it to behave in a manner similar to a spring mass damper system which exhibits oscillatory behaviour following any disturbance from the equilibrium state.

Small oscillations were a matter of concern, but for several decades power system engineers remained preoccupied with transient stability. That is the stability of the system following large disturbances. Causes for such disturbances were easily identified and remedial measures were devised. In the early sixties, most of the generators were getting interconnected and the automatic voltage regulators were more efficient. With bulk power transfer on long and weak transmission lines and application of high gain fast acting AVRs, small oscillations of even low frequency were observed. These were described as inter-tie oscillations. Some times oscillations of the generators within the plant were also observed. These oscillations at slightly higher frequency were termed as Intra plant oscillations.

The combined oscillatory behaviour of the system encompassing the three modes of oscillations are popularly called the dynamic stability of the system. In more precise terms it is known as the small signal oscillatory stability of the system.

The oscillations, which are typically in the frequency range of 0.2 to 0.3 Hz, might be excited by disturbances in the system or, in some cases, might even build up spontaneously. These oscillations limit the power transmission capability of a network and sometimes, may even cause loss of synchronism and an eventual breakdown of the entire system. In practice, in addition to stability, the system is required to be well damped i.e the oscillations, when excited, should die down within a reasonable amount of time. [5, 14]

The stability of the system, in principle, can be enhanced substantially by application of some form of closed loop feedback control. Over the years a considerable amount of effort has been extended in laboratory research and on site studies for designing such controllers.

1.3 Criteria for damping

The rate of the decay of the amplitude of oscillations is best described in terms of damping ratio ζ . For an oscillatory mode represented by $-\sigma + j\omega$, the damping ratio is given by

$$\zeta = \frac{-\sigma}{\sqrt{(\sigma^2 + \omega^2)}} \quad (1.1)$$

The damping ratio determines the rate of the decay of the amplitude of oscillation. The time constant of amplitude decay is $\frac{1}{|\sigma|}$. In other words amplitude decays to $\frac{1}{e}$, 37% of its initial amplitude in $\frac{1}{|\sigma|}$ seconds or $\frac{1}{2\pi\zeta}$ cycles of oscillation. As oscillatory mode having a wide range of oscillations, the use of damping ratio ζ rather than the time constant of decay is considered more appropriate for expressing the degree of damping. For example, a 5-sec time constant represents amplitude decay to 37% of initial value in 110 cycles of oscillation for a 22 Hz torsional mode, in 5 cycles for a 1-Hz local plant mode, and in one-half cycle for a 0.1-Hz interarea mode of oscillation. On the other hand, a damping ratio of 0.032 represents the same degree of

amplitude decay in 5 cycles, for example, for all modes. A power system should be designed and operated so that the following criteria are satisfied for all expected system conditions, including post-fault conditions following design contingencies

The damping ratio (ζ) of all system modes oscillation should exceed a specified value. The minimum acceptable damping ratio is system dependent and is based on operating experience and/or sensitivity studies, it is typically in the range 0.03–0.05. [14]

1.4 Literature review

Concordia *et al.* [1] have presented the phenomena of stability of synchronous machines under small perturbations by examining the case of a single machine connected to an infinite bus through external reactance. The analysis develops insights into effects of thyristor type excitation systems and establishes understanding of the stabilizing requirements for such systems. Bacalao *et al.* [3] have studied the application of a numerical optimization scheme to the tuning of power system stabilizers. The scheme is based on minimax optimization techniques with multiple objectives given by relevant system perturbations, aggregated by means of a weighted sum. Champagine *et al.* [4] have proposed a uncommon structure for the PSS transfer function to improve the damping of the system low frequency, as well as the usual local and interarea frequencies. These somewhat conflicting goals are achieved by adding the speed-based stabilizing signals of two compensation filters, which independently provide the phase adjustment necessary for adequate damping torques at two widely separated center frequencies. Lawson *et al.* [7] have proposed a basic theory of a PSS control based on integral of accelerating power input signal and the methods of tuning the stabilizer. Small signal linearized analysis using frequency domain techniques (bode plots and root locus) are used to illustrate the process of tuning the PSS controls. Abdel-Magid *et al.* [10] have demonstrates the robust tuning of power systems stabilizers for power systems, operating at different loading conditions. A classical lead-lag power system stabilizer is used to demonstrate the technique. The problem of selecting the stabilizer parameters is converted to a simple optimization problem with an eigenvalue-based objective function, which is solved by a tabu search algorithm. The effectiveness of the stabilizers tuned using the suggested technique, in enhancing the stability of power systems, is confirmed through

eigenvalue analysis and simulation results. Abido [11] has presented robust design of multimachine power system stabilizers (PSSs) using simulated annealing (SA) optimization technique. The proposed approach employs SA to search for optimal parameter settings of a widely used conventional fixed-structure lead-lag PSS (CPSS). One of the main advantages of the proposed approach is its robustness to the initial parameter settings. In addition, the quality of the optimal solution does not rely on the initial guess. The performance of the proposed SAPSS under different disturbances and loading conditions is investigated for two multimachine power systems. Abido *et al.* [12] have presented robust design of multimachine power system stabilizers (PSSs) using the tabu search (TS) optimization technique. The proposed approach employs TS for optimal parameter settings of a widely used conventional fixed-structure lead-lag PSS (CPSS). Incorporation of TS as a derivative-free optimisation technique in PSS design significantly reduces the computational burden. In addition, the quality of the optimal solution does not rely on the initial guess. Abdel-Magid *et al.* [13] proposed the optimal design of power system stabilizers (PSSs) using evolutionary programming (EP) optimization technique. The proposed approach employs EP to search for optimal settings of PSS parameters that shift the system eigenvalues associated with the electromechanical modes to the left in the s-plane. The eigenvalue analysis and the nonlinear simulation results show the effectiveness and robustness of the proposed PSSs to damp out the local as well as the interarea modes of oscillations and work effectively over a wide range of loading conditions and system configurations. Abdel-Magid *et al.* [15] have presented a optimal multiobjective design of robust multimachine power system stabilizers using genetic algorithms. A multiobjective problem is formulated to optimize a composite set of objective functions comprising the damping factor, and the damping ratio of the lightly damped electromechanical modes. The problem of robustly selecting the parameters of the power system stabilizers is converted to an optimization problem which is solved by a genetic algorithm with the eigenvalue based multiobjective function.

Monavar *et al.* [16] proposed simultaneous placement and tuning of power system stabilizers for stabilization of power systems over a wide range of operating conditions using genetic algorithm. A PSS tuned using this procedure is robust at different operating conditions and structure changes of the system. Dubey *et al.* [19]

have presented a systematic approach for the design of power system stabilizer using genetic algorithm and investigates the robustness of the GA based PSS. The proposed approach employs GA search for optimal setting of PSS parameters. The performance of the proposed GPSS under small and large disturbances, loading conditions and system parameters is tested. The eigenvalue analysis and nonlinear simulation results show the effectiveness of the GPSS to damp out the system oscillations Gurrala *et al.* [21] have derived a modified Heffron- Phillips (K- constant model) model for the design of power system stabilizers. In the proposed method, information available at the secondary bus of the step-up transformer is used to set up a modified Heffron- Phillip's (ModHP) model. The PSS design based on this model utilizes signals available within the generating station. The efficacy of the proposed design technique and the performance of the stabilizer has been evaluated over a range of operating and system conditions. Zellagui [22] has proposed genetic local search technique which hybridizes the genetic algorithm and the local search (such as hill climbing) in order to eliminate the disadvantages in genetic algorithm. The parameters of the power system stabilizer are tuned by considering the single machine connected to infinite bus system. The eigen value analysis shows that the proposed GLSPSS based PSS has better performance compared with conventional and genetic based PSS. Al –Hinai *et al.* [25] have analyzed the dynamics of a single machine connected to infinite bus power system. Such analysis requires a certain level of system modeling. The main system components models are the synchronous machine, excitation system and the Power System Stabilizer. The Matlab/Simulink is used as a programming tool to analyze the system performance. According to the system performance a proper design for the Power System Stabilizer (PSS) using Particle Swarm Optimization (PSO) is carried out. Then the designed PSS is implemented in the model and the dynamic system response is analyzed. Since the simulation results without the PSS showed unacceptable system response, the system response with the PSS has improved and the PSS succeeded to stabilize an unstable system.

Eberhart *et al.* [6] have introduced a concept for the optimization of nonlinear functions using particle swarm methodology. Benchmark testing of the paradigm is described, and applications, including nonlinear function optimization and neural network training, are proposed. The relationships between particle swarm optimization and both artificial life and genetic algorithms are described. Eberhart *et*

al. [9] empirically study the performance of the particle swarm optimizer (PSO). Four different benchmark functions with asymmetric initial range settings are selected as testing functions. The experimental results illustrate the advantages and disadvantages of the PSO. Ma *et al.* [17] A PSO with increasing inertia weight, distinct from a widely used PSO with decreasing inertia weight, is proposed in this paper. Four standard test functions with asymmetric initial range settings are used to confirm its validity. From the experiments, it is clear that a PSO with increasing inertia weight outperforms the one with decreasing inertia weight, both in convergent speed and solution precision, with no additional computing load compared with the PSO with a decreasing inertia weight. Moore *et al.* [20] have introduced unconstrained modified particle swarm optimization (UMPSO) algorithm and study empirically. Four well known benchmark functions, with asymmetric initial position values, are used as testing functions for the UMPSO algorithm. The UMPSO is a variation of the canonical PSO in which the velocity and position is unconstrained, an additional strategic component is added, and the social component term has been modified. Liu *et al.* [24] have presented hierarchical structure poly-particle swarm optimization (HSPPSO) approach using the hierarchical structure concept of control theory. The test of proposed method on four typical functions shows that HSPPSO performance is better than PSO both on convergence rate and accuracy.

1.5 Scope of the present work

The objective of the present work is to show that even a properly tuned fixed parameter controller can guarantee a robust minimum performance over a wide range of operating conditions. Since fixed parameter PSS is a simple in structure and widely used by most utilities, an attempt is made to tune the fixed parameter PSS to ensure its robustness.

PSO has been applied for robust PSS design, which includes several operating conditions and system configurations simultaneously in the design process and works well with equal effectiveness in single machine environment. PSS parameters are obtained using Particle swarm optimization algorithm.

1.6 Organization of the thesis

In Chapter 1 a brief overview of dynamic stability is given. A detailed information about power system oscillations, its historical perspective, remedial measures and low frequency oscillations is discussed. Further brief literature review and scop of the present work is presented.

In Chapter 2 a brief introduction of small signal stability of single machine infinite bus system is discussed. Further the need of PSS is elaborated. Tuning guidelines of conventional power system stabilizer, and through it CPSS parameters are obtained. Simulation study and torque characteristic is shown to justify the need of PSS.

In Chapter 3 introduction of particle swarm optimization is presented. Further basic particle swarm optimization is discussed through its step by step algorithm and flow chart is drawn. A test example is shown to check the effectiveness of PSO.

In Chapter 4 Problem formulation is discussed.

In Chapter 5 optimized parameters are obtained through PSO technique. Results are discussed, summary is concluded.

CHAPTER#2

SMALL SIGNAL STABILITY OF A SMIB SYSTEM

2.1 Introduction

The subsystems of power systems are described by (a) complex and (b) nonlinear models, in fact even single dynamic representation of single generator infinite bus system (the classical swing equation model) is nonlinear. The consequence of this is that for appreciable disturbances the characteristics of the system's response (and hence whether the system is stable) is different at each operating point and for every disturbance. This class of power system stability – where the non-linearities of the system cannot be ignored, and the consequent requirement is that we can only make stability judgements for specific contingencies – is referred to as *transient stability*.

Conversely, there is another class of power system stability for which the non-linear characteristics of the system can be ignored with minimal error in the predicted response, this class is referred to as *small-signal stability* and it is concerned with the ability of the system to remain in synchronism (stable) following *small* disturbances.

Whether or not a disturbance is sufficiently small is determined by the degree of non-linearity of the system, which itself will change with operating point. Hence there is no definitive answer except to say that the disturbance must obviously be small enough to ensure that representing the system with a linearized model is reasonable. This in itself requires skill and experience, and one must always be sure to check any predictions made on the basis of linearized approximations to the full model against the predictions of the full model itself. certain categories of power system behaviour / phenomena are known) to fall in the category small-signal stability. Local and inter-area oscillations (insufficient damping), subsynchronous resonance and stability of control mode are few of them. [5]

2.2 Synchronous machine model

The synchronous machine is vital for power system operation. The general system configuration of synchronous machine connected to an infinite bus through transmission network can be represented as the Thevenin's equivalent circuit shown in figure 2.1 [5]

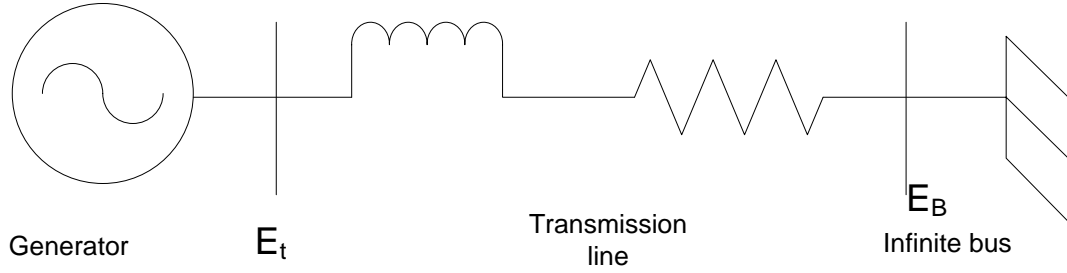


Fig 2.1 The equivalent circuit of synchronous machine connected to infinite bus system

2.3 Classical model

The generator is represented as the voltage E' behind X_d' as shown in Fig 2.2. The magnitude of E' is assumed to remain constant at the pre-disturbance value. Let δ be the angle by which E' leads the infinite bus voltage E_B . The δ changes with rotor oscillations. The line current is expressed as-

$$I_t = \frac{E' \angle 0^\circ - E_B \angle -\delta}{jX_T} \quad (2.1)$$

The complex power behind X_d' is given by

$$\begin{aligned} S' &= P + jQ = E' I_t^* \\ &= \frac{E' E_B \sin \delta}{X_T} + j E' \left(\frac{E' - E_B \cos \delta}{X_T} \right) \end{aligned} \quad (2.2)$$

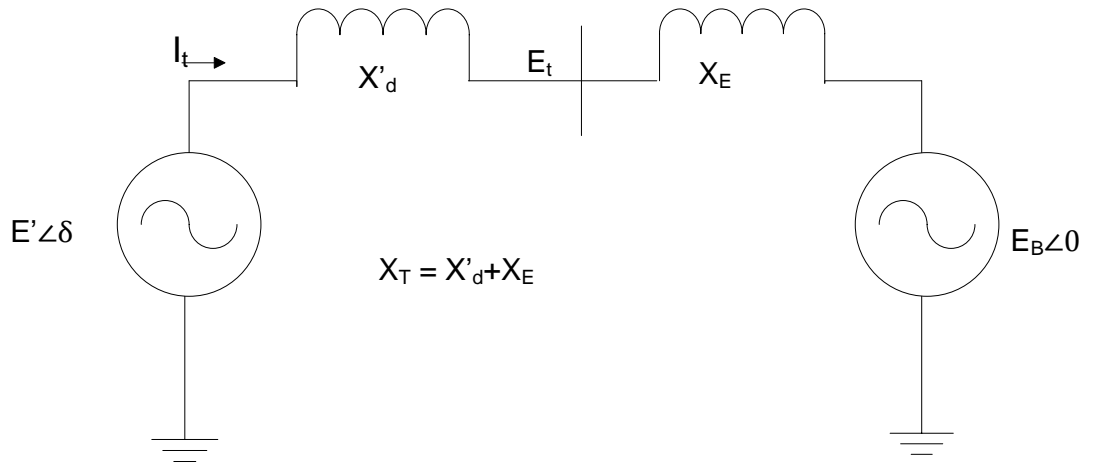


Fig. 2.2 Classical model of generator

With the stator resistance neglected the airgap power (P_e) is equal to the terminal power (P). In per unit airgap torque is equal to airgap power. Hence

$$T_e = P = \frac{E' E_B}{X_T} \sin \delta \quad (2.3)$$

Linearizing about an initial operating condition represented by $\delta = \delta_0$ yields –

$$\Delta T_e = \frac{\partial T_e}{\partial \delta} \Delta \delta = \frac{E' E_B}{X_T} \cos \delta_0 (\Delta \delta) = K_s \Delta \delta \quad (2.4)$$

Where

$$K_s = \frac{E' E_B}{X_T} \cos \delta_0$$

The equations of motion in per unit are-

$$P \Delta \omega = \frac{1}{2H} (T_M - T_e - K_D \Delta \omega_r) \quad (2.5)$$

$$P \delta = \omega_0 \Delta \omega_r \quad (2.6)$$

Where $\Delta\omega_r$ is the per unit speed deviation, δ is the rotor angle in electrical radians, ω_0 is the base rotor electrical speed in radians per second and P is the differential operator $\frac{d}{dt}$ with time t in seconds.

Linearizing equation 2.5 and substituting for ΔT_e given by Equation 2.4, results into

$$P\Delta\omega_r = \frac{1}{2H}(\Delta T_m - K_s\Delta\delta - K_D\Delta\omega_r) \quad (2.7)$$

$$P\Delta\delta = \omega_0\Delta\omega_r \quad (2.8)$$

Writing equations 2.7 & 2.8 in matrix form

$$\frac{d}{dt} \begin{bmatrix} \Delta\omega_r \\ \Delta\delta \end{bmatrix} = \begin{bmatrix} -\frac{K_D}{2H} & -\frac{K_s}{2H} \\ \omega_0 & 0 \end{bmatrix} \begin{bmatrix} \Delta\omega_r \\ \Delta\delta \end{bmatrix} + \begin{bmatrix} 1/2H \\ 0 \end{bmatrix} \Delta T_m \quad (2.9)$$

The equation 2.9 is of the form $Px = Ax + Bu$. The elements of the state matrix A are seen to be dependent on the system parameters K_D , H , K_s , and the initial operating condition represented by the value of E' and δ_0 . The equation 2.9 to describe small-signal performance is represented in block diagram as Fig. 2.3.

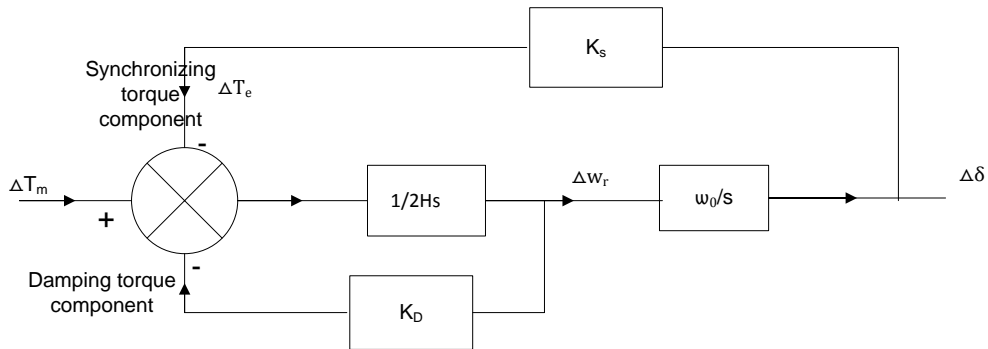


Fig. 2.3 Block diagram of single machine infinite bus system with classical model.

K_s = Synchronizing torque coefficient in pu torque/rad

K_D =Damping torque coefficient in pu torque/pu speed deviation

H = Inertia constant in MW.s/MVA

ω_0 = Rated speed in elec.rad/s = $2\pi f_0 = 314$ for a 50 Hz system

$\Delta\omega_r$ = Speed deviation in per unit = $\frac{(\omega_r - \omega_0)}{\omega_0}$

s = Laplace operator

$\Delta\delta$ = Rotor angle deviation in elec.rad

This diagram illustrates graphically the concept of synchronizing and damping torques central to small-signal stability. If the system is disturbed by (for eg.) changing the mechanical input torque (ie. T_m becomes non-zero) there are two types of opposing torques that are developed

An opposing torque in phase with load angle deviation (at the output of block K_s).

An opposing torque in phase with speed deviation (at the output of block K_D).

From the block diagram we have

$$\Delta\delta = \frac{\omega_0}{s} \left(\frac{1}{2Hs} (-K_s \Delta\delta - K_D \Delta\omega_r + \Delta T_m) \right) \quad (2.10)$$

$$= \frac{\omega_0}{s} \left(\frac{1}{2Hs} \left(-K_s \Delta\delta - K_D s \frac{\Delta\delta}{\omega_0} + \Delta T_m \right) \right) \quad (2.11)$$

Solving the block diagram we get the characteristic equation

$$s^2 + \frac{K_D}{2H} s + \frac{K_s}{2H} \omega_0 = 0 \quad (2.12)$$

Comparing it with general form, the undamped natural frequency ω_n and damping ratio ξ are expressed as

$$\omega_n = \sqrt{\frac{K_s \omega_0}{2H}} \quad (2.13)$$

$$\zeta = \frac{K_D}{2\sqrt{(K_s 2H\omega_0)}} \quad (2.14)$$

Equation 2.13 & 2.14 tell us the natural frequency and damping factor of the oscillations that result from a small disturbance to the system at a particular operating point. As the synchronizing torque coefficient K_s increases, the natural frequency increases and the damping ratio decreases. An increase torque coefficient K_D increases the damping ratio, where as an increase in inertia constant decreases both natural frequency and damping ratio.

2.4 Variable voltage (E'_q) behind transient reactance (X'_d) model – no AVR

Now we add the field circuit dynamic equation into the non-linear model and re-linearise to get the following small-signal model [5]

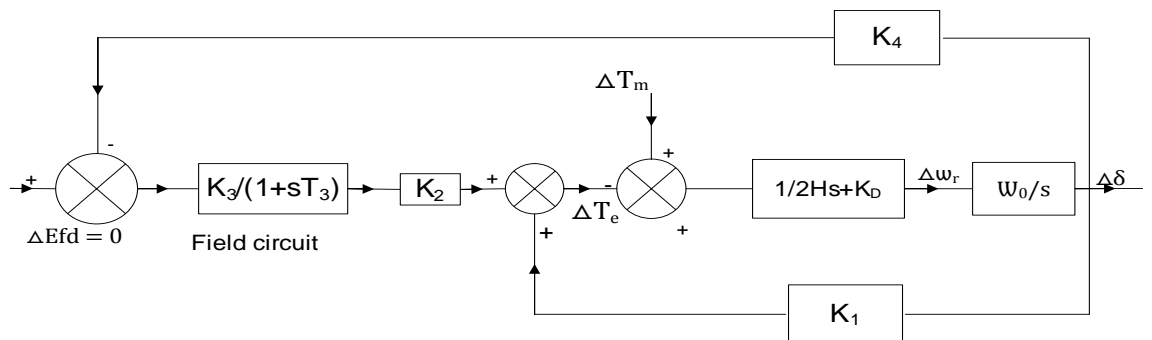


Fig. 2.4 Block diagram representation with constant E_{fd}

Figure 2.4 shows the block diagram representation of the small signal performance of the system. In this representation, the dynamic characteristic of the system are expressed in terms of the K constants. The model is the basis for the the Phillips-Heffron linear model [1] of a synchronous machine and it is widely used to analyse the impact of excitation control on system stability.

Where

$$K_1 = \frac{\Delta T_e}{\Delta \delta}, \text{ for constant } E'_q$$

change in electrical torque for a change in rotor angle with constant flux linkages in the d axis.

$$K_2 = \frac{\Delta T_e}{E'_q}, \text{ for constant } \delta$$

change in electrical torque for a change in d-axis flux linkages with constant rotor angle.

$K_3 =$ Impedance factor.

$$K_4 = \frac{1}{K_3} \frac{E'_q}{\Delta \delta}$$

Demagnetizing effect of change in rotor angle.

For the special case of zero external resistance the expressions of the K constants of synchronous machine becomes

$$K_1 = \frac{E_{q0} V_b}{X_{qT}} \cos \delta_0 + \frac{(X_q - X'_d)}{X_{dT'}} i_{q0} V_b \sin \delta_0 \quad (2.15)$$

$$K_2 = \frac{V_b}{X_{dT'}} \sin \delta_0 \quad (2.16)$$

$$K_3 = \frac{X_{dT'}}{X_{dT}} \quad (2.17)$$

$$K_4 = \frac{(X_d - X'_d)}{X_{dT'}} V_b \sin \delta_0, \quad (2.18)$$

$$T_3 = K_3 T'_{d0}, \quad (2.19)$$

and where

$$X_{dT'} = X'_d + X_E$$

$$X_{dT} = X_d + X_E$$

$$X_{qT} = X_q + X_E$$

Increasing the load angle (ie. making a positive deviation $\Delta\delta$) increases the misalignment of stator and rotor fluxes, thus changing the flux that links the rotor (field). From Faraday's Law, we understand that change in flux = induced emf. From these basic physical understandings, two important dependencies can be seen, the larger the initial load angle $\Delta\delta$, the larger the change in rotor flux should be for a given deviation in load angle and hence the larger the induced voltages and currents in the field. By demagnetising the field as a result of a deviation in rotor angle, we are reducing the amount of counter torque that can be produced by virtue of this deviation because of the reduced size of the field magnetisation, this slight demagnetisation of the field due to a deviation in angle reduces the synchronising torque slightly from the case when the field flux is assumed to remain constant.

If we disturb the system by means of a small increase in mechanical input torque ($\Delta T_m = +ve$). The restorative (stabilizing) electrical counter torques developed by the machine in response come via two channels. The output of block K_1 is a pure synchronising torque whose magnitude is operating point dependent. The output of block K_2 is comprised of both synchronising and damping components of torque, but each of these are operating point dependent. Considering torque deviations due to field effects only

$$\frac{\Delta T_e}{\Delta\delta} \text{ due to } \psi_{fd} = \frac{-K_2 K_3 K_4}{(1 + sT_3)} \quad (\text{with } K_2, K_3 \& K_4 \text{ usually positive}) \quad (2.20)$$

Because of the field circuit dynamics (field time constant) the output ΔT_e is frequency dependent. There are three important frequencies to consider

(i) Steady- state ($s = j\omega = 0$)

$$\Delta T_e \text{ due to } \psi_{fd} = -K_2 K_3 K_4 \Delta\delta \quad (2.21)$$

There will be negative impact of armature reaction on synchronising torque. Steady-state stability limit when $K_1 - K_2 K_3 K_4$ decreases to zero. Armature reaction purely affects synchronism at steady state. When $K_1 - K_2 K_3 K_4 \leq 0$, monotonic instability (drifting)

(ii) Very high oscillating frequencies ($s = j\omega \gg 1/T_3$)

$$\frac{\Delta T_e}{\Delta \delta} \text{ due to } \psi_{fd} = -K_2 K_3 K_4 \Delta \delta \frac{1}{j\omega T_3} = K_2 K_3 K_4 j \Delta \delta \frac{1}{\omega T_3} \quad (2.22)$$

ΔT_e due to ψ_{fd} 90° ahead of $\Delta \delta$, ie. In phase with $\Delta \omega$, +ve damping torque.

(iii) Typical rotor oscillation frequency (1 Hz)

ΔT_e due to ψ_{fd} exhibits Small negative component in phase with $\Delta \delta$. Positive component in phase with $\Delta \omega$. The net effect is then

$$K_s = K_1 + K_s | \text{due to } \psi_{fd} \quad (2.23)$$

$$K_D = K_D | \text{due to } \psi_{fd} \quad (2.24)$$

It is useful to compare the small-signal characteristics of a SMIB system as predicted by the classical model (no electrical dynamics) with the characteristics of a SMIB system as predicted by the variable voltage behind transient reactance model (field circuit dynamics represented), as this enables us to isolate the effect of field flux variations on small-signal stability

It is not (usually) possible for the system to become unstable due to lack of damping with constant field voltage. As the load angle increases and the net synchronising torque coefficient decreases the system becomes prone to drift off from its steady state operating point – this drifting instability has virtually been eliminated in modern power systems with the introduction of excitation control (AVRs).

As the load angle increases, the damping contribution due to $\Delta \psi_{fd}$ increases. Thus as a system becomes closer to its transient stability limit it can become more stable with respect to damping.

2.5 Variable voltage ($E_{q'}$) behind transient reactance ($X_{d'}$) model – with exciter and AVR

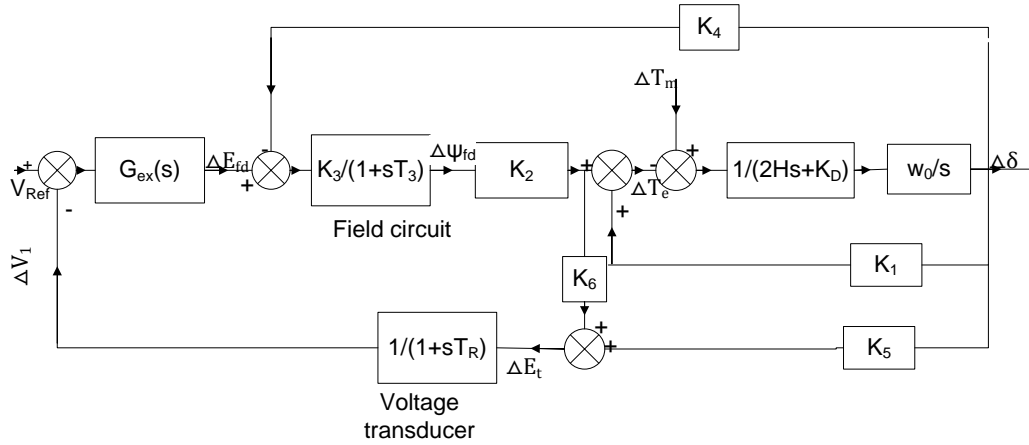


Fig. 2.5 AVR BLOCK diagram representation with exciter and AVR

On same machine model, external controller is connected. The exciter can be any one of a number of types but here we assume it is a high-gain thyristor type exciter for which $G_{ex}(s) = K_A$.

Also,

$$K_5 = -\frac{X_q V_{d0}}{X_{qT} V_{t0}} V_b \cos \delta_0 - \frac{X'_d V_{q0}}{X_{dT'} V_{t0}} V_b \sin \delta_0 \quad (2.25)$$

$$K_6 = \frac{X_E V_{q0}}{X_{dT'} V_{t0}} \quad (2.26)$$

The model is now fairly complex. It is useful first to see what can be understood conceptually from the block diagram of the linearised model itself. The introduction of the AVR means field flux variations are now caused by both armature reaction and field voltage variations. The expressions for K_5 and K_6 illustrate that the performance of the AVR will vary with operating conditions, and therefore the tuning of the AVR needs thought. The effect of the AVR will clearly be to alter both synchronising and damping torques.

From experience it has been found that while K_2 , K_3 , K_4 and K_6 are usually positive, K_5 can be positive or negative. With K_5 positive, the effect of AVR is to introduce a negative synchronizing torque and a positive damping torque component. The constant K_5 is positive for low values of external system reactance and low generator outputs. With K_5 negative, the AVR action introduces a positive synchronizing torque component and a negative damping torque component.

For high values of external system reactance and high generator outputs K_s is negative. In practice, the situation where K_s is negative are commonly encountered. For such cases, a high response exciter is beneficial in increasing synchronizing torque. However, in doing so it introduces a negative damping. We thus have conflicting requirements with regard to exciter response. One possible recourse is to strike a compromise and set the exciter response so that it results in sufficient synchronizing and damping torque components for the expected range of system operating conditions. This may not be always possible. It may be necessary to use a high response exciter to provide the required synchronizing torque and transient stability performance. With a very high external system reactance, even with low exciter response the net damping torque coefficient may be negative [5].

An effective way to meet the conflicting exciter performance requirements with regard to system stability is to provide a *power system stabilizer*.

2.6 Power system stabilizer

The basic function of power system stabilizer is to add damping to the generator rotor oscillations by controlling its excitation using auxiliary stabilizing signal(s). To provide damping stabilizer must produce a component of electrical torque in phase with the rotor speed deviations.

The theoretical basis for a pss may be illustrated with the aid of block diagram shown in fig. 2.6. This is an extension of block diagram of fig. 2.5 and include the effects of PSS.

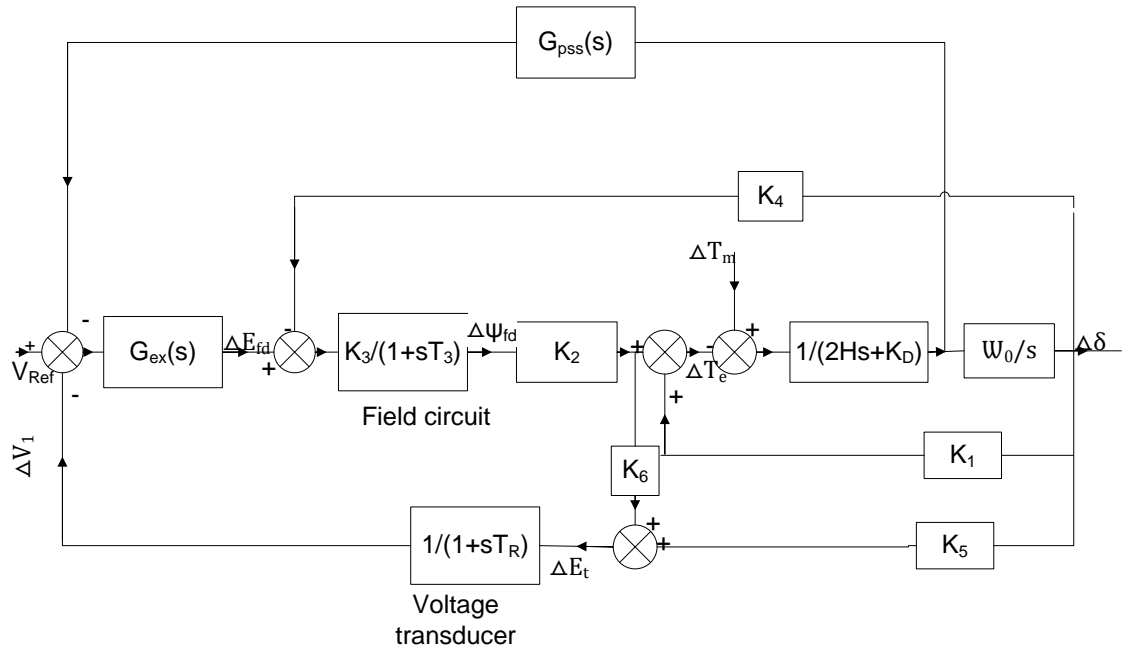


Fig. 2.6 Block diagram representation with AVR and PSS.

Since the purpose of PSS is to introduce a damping torque component, a logical signal to use for controlling generator excitation is the speed deviation $\Delta\omega_r$.

If the exciter transfer function $G(s)$ and the generator transfer function between exciter input and electrical torque were pure gains, a direct feedback of speed deviation would result in damping torque. However both the generator and exciter (depending on its type) exhibit frequency dependent gain and phase characteristic. Therefore, the PSS transfer function, $G_{PSS}(s)$, should have phase compensation circuits to compensate for the phase lag between exciter input and electrical torque. In the ideal case, the phase characteristic of $G_{PSS}(s)$ being an exact inverse of the exciter and generator phase characteristics to be compensated, the PSS would result in pure damping torque for all oscillating frequencies.

The following is a brief description of the basis for the PSS configuration and consideration in selection of parameters

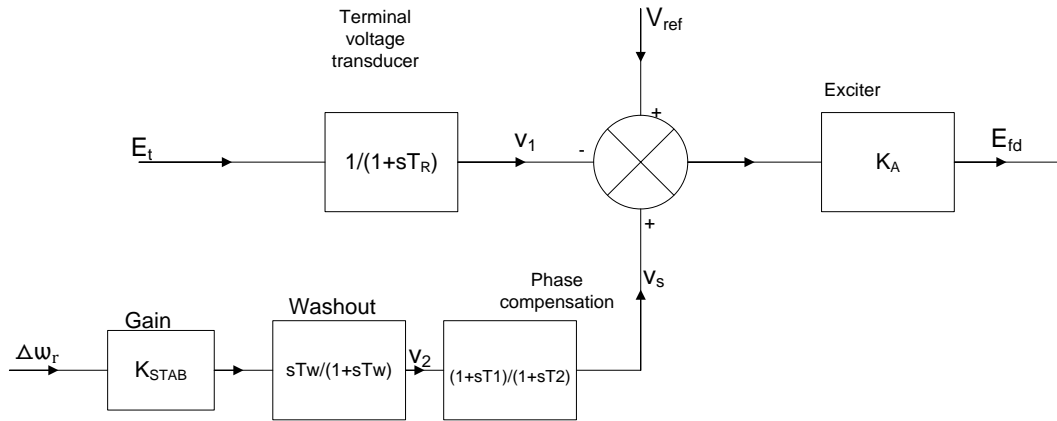


Fig. 2.7 Thyristor excitation system with AVR and PSS

The phase compensation block provides the appropriate phase lead characteristics to compensate for the phase lag between exciter input and generator electrical torque. The phase compensation may be a single first order block as shown in Fig.2.7 or having two or more first order blocks or second order blocks with complex roots.

The signal washout block serves as high pass filter, with time constant T_w high enough to allow signals associated with oscillations in ω_r to pass unchanged, which removes d.c. signals. Without it, steady changes in speed would modify the terminal voltage. It allows PSS to respond only to changes in speed.

The stabilizer gain K_{STAB} determines the amount of damping introduced by PSS. Ideally, the gain should be set at a value corresponding to maximum damping, however, it is limited by other consideration.[5]

2.7 Tuning Guidelines for the CPSS

The conventional, lead compensation type of PSS continues to be the most popular with the industry due to its simplicity and well understood operational principles.

Consider the Heffron-Philips model of the SMIB system shown in fig.2.8. It is required to inject a signal derived from the rotor speed at the AVR voltage reference input such that a damping component of the electrical torque is generated. As seen, the stabilizing signal passes through a part of the system before arriving at the torque summing junction. This subsystem termed as GEP(s) is shown by the colored outline line as shown in fig. 2.8. The signal suffers a phase lag due to this block. Fig. 2.9

shows a typical magnitude plot and phase angle plot of the transfer function of the $GEP(s)$ at the oscillating frequency. For the signal at the output of the $GEP(s)$ to be in the phase with rotor speed it is necessary to provide a phase lead to the injected signal equal to the phase lag of the block $GEP(s)$ at the oscillating frequency. Fig. 2.10 shows a phase plot of such a lead compensator $PSS(s)$ and fig. 2.11 shows the resulting compensated phase angle of the cascade $GEP(s).PSS(s)$. [14]

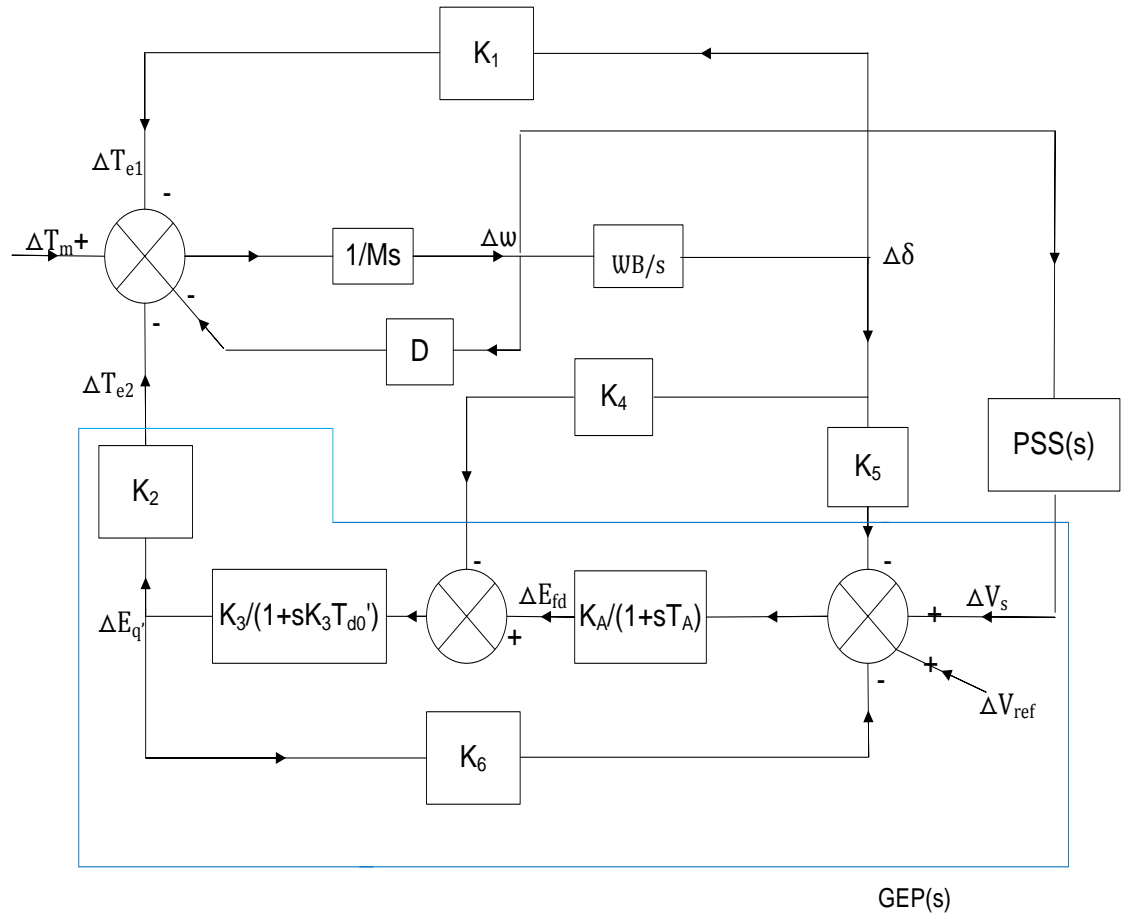


Fig. 2.8 Heffron- Phillips model of the SMIB System

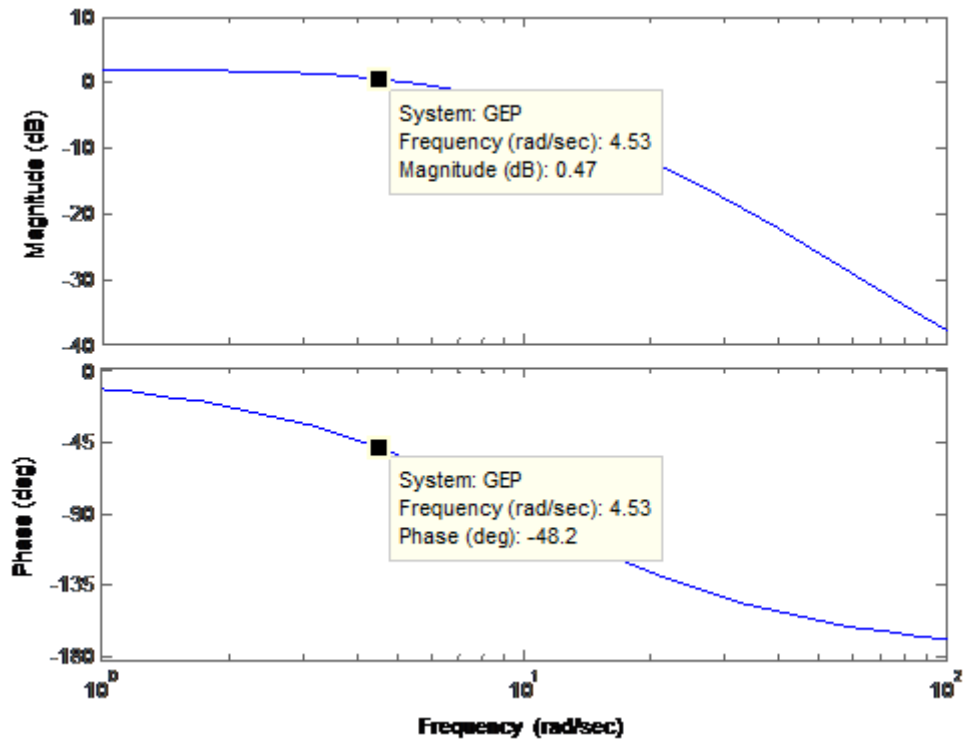


Fig. 2.9 Magnitude and phase plot of transfer function GEP(s)

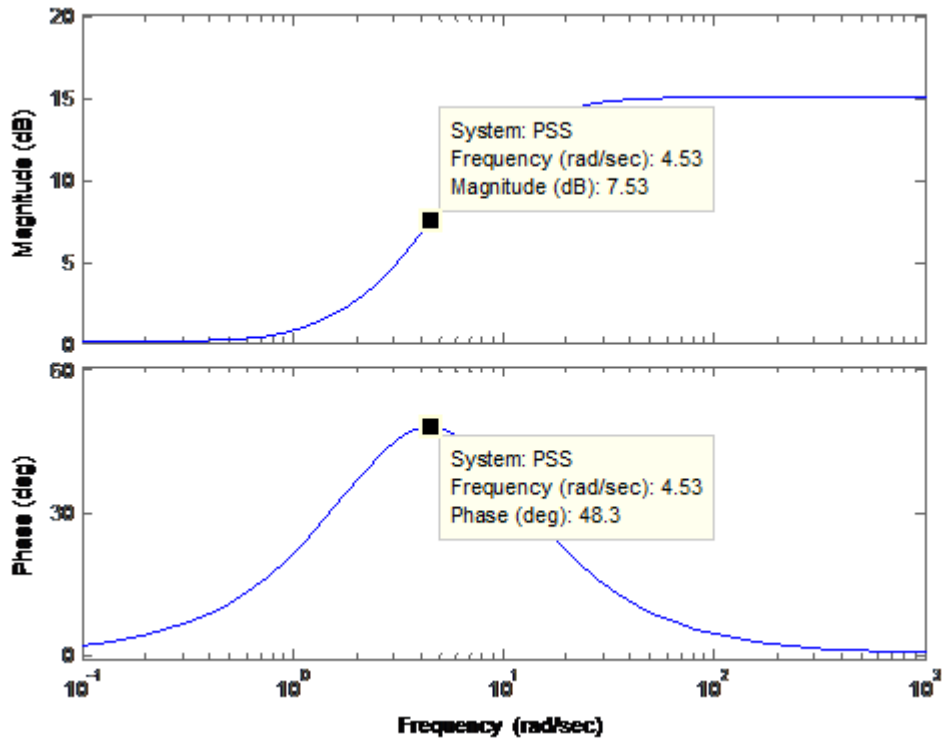


Fig. 2.10 Magnitude and phase plot of transfer function PSS(s)

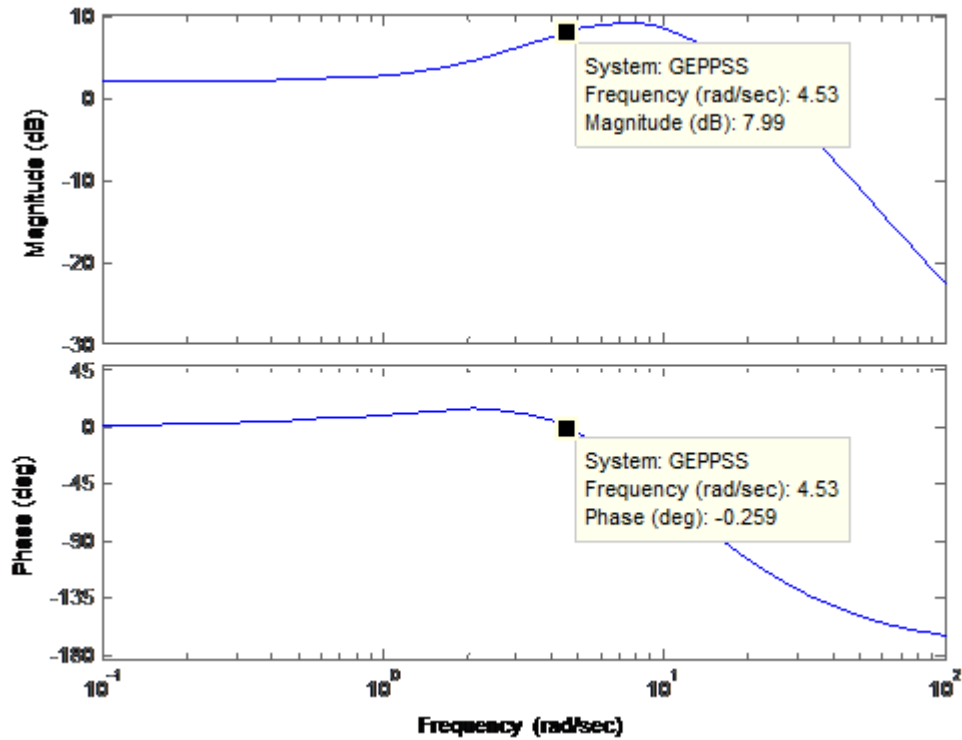


Fig. 2.11 Magnitude and phase plot of transfer function GEP(s).PSS(s)

The transfer function of the lead compensator is taken as

$$PSS(s) = K_s \frac{(1 + sT_1)(1 + sT_1)}{(1 + sT_2)(1 + sT_2)} \quad (2.27)$$

A value of the compensated phase angle of GEP(s).PSS(s) between 0 and -90 degrees results in additional damping. Overcompensation results in a decrement of the net synchronizing torque and hence should be avoided. For a practical implementation, it is recommended to keep the phase angle of GEP(s).PSS(s) between 0 and -40 degrees at the oscillating frequency and between 0 and -90 degrees over a wide frequency range as possible. The compensator parameters T_1 and T_2 are chosen so as to maintain the phase angle of the GEP(s).PSS(s) within these limits.

The root locus of the system with chosen lead compensator is then plotted. The gain of the PSS is chosen such that the damping of the rotor mode eigen value is thus maximized. If any other modes (like the exciter mode) tend to get destabilized with an increase in the gain, the damping of these modes is also considered. [14]

The transfer function of the GEP(s) is given as

$$\text{GEP}(s) = \frac{(K_2 K_3 K_A)}{(1 + sT_A)(1 + sT'_{do}) + k_3 k_6 K_A} \quad (2.28)$$

2.8 Magnitude requirements

Referring to the torque angle characteristic equation

$$s^2 + \frac{K_D}{2H}s + \frac{K_s}{2H}\omega_0 = 0$$

Where K_D describes the gain of the damping term, $\frac{\Delta T_D}{\Delta \omega_r}$, we note that

$$\omega_n = \sqrt{\frac{K_s \omega_0}{2H}}$$

and

$$\zeta = \frac{K_D}{2\sqrt{(2K_s H \omega_0)}}$$

for a constant damping ratio we have

$$K_D = 2\zeta\sqrt{2K_s H \omega_0} = 2M\zeta\sqrt{\frac{K_s \omega_0}{2H}} = 2\zeta M \omega_n$$

The magnitude of the signal that would be required would then be $A2\zeta M \omega_n$ where A is the reciprocal of the magnitude of the function $\text{GEP}(s)$ at the oscillating frequency.

2.9 Operating conditions

The operating condition for the system is completely defined by the values of real power P , the reactive power Q , at the generator terminals and the equivalent transmission line impedance X_e .

2.10 CPSS Parameter selection

The operating point corresponding to $P = 0.9$, $Q = 0.1$, $X_e = 0.977$ was chosen as nominal operating point. The CPSS is designed for this nominal operating point using the tuning guidelines already discussed in 2.7.

At the undamped natural oscillating frequency of ω_n (4.53 rad/sec) the chosen lead compensator parameters are $T_1 = 0.3406$, $T_2 = 0.1430$

Stabilizer gain at the oscillating frequency is given by

$$K_s = 2\zeta A M \omega_n = 9.962$$

Where $\zeta = 0.3$ and A is the reciprocal of the magnitude of GEP(s) at oscillating frequency.

2.10.1 Eigenvalues

The eigenvalues of the system without and with PSS are shown below in the table 2.1

Without PSS	With PSS
0.2562 - 4.7490i, 0.2562+4.7490i	-6.9930 , -15.3832 , -0.6274 + 5.1555i
-10.3631 + 1.8344i, -10.3631 - 1.8344i	-0.6274 - 5.1555i, -5.2841 + 3.7504i, -5.2841 - 3.7504i, -0.1006

Table 2.1 Eigenvalues of the system without and with PSS

2.10.2 Damping

$$\zeta = \frac{-\sigma}{\sqrt{(\sigma^2 + \omega^2)}}$$

Clearly the damping is negative in the case without PSS.

$$\zeta = -.053$$

In the case with PSS damping seems to be positive and the stability of the system is enhanced.

$$\zeta = 0.1208$$

2.11 Simulation study

Time domain performance of the system without and with PSS are shown below. System response is in the form of speed deviation ($\Delta\omega_r$), load angle ($\Delta\delta$), and terminal voltage (V_t). The disturbance are given at $t = 1$ sec. A unit step change is considered in input mechanical torque. The power system model is simulated for 10 seconds.

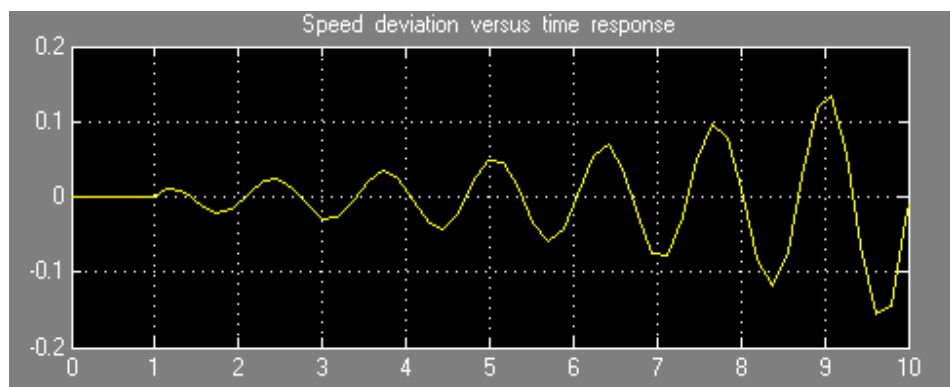


Fig (a)

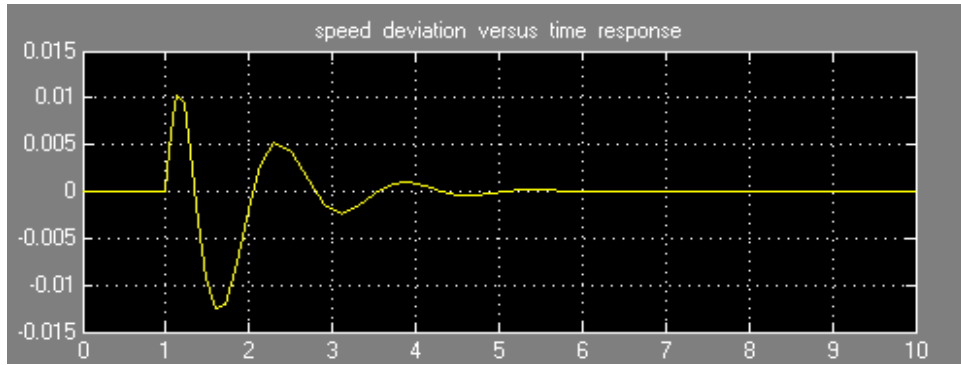


Fig (b)

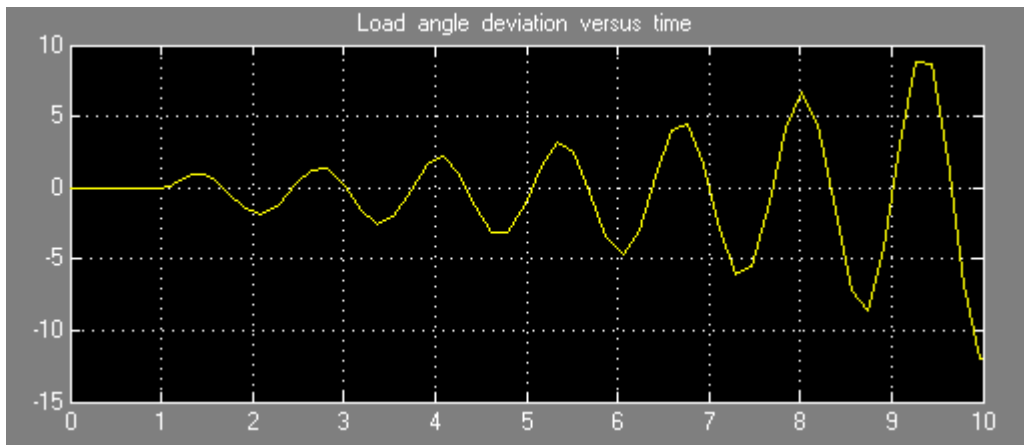


Fig (c)

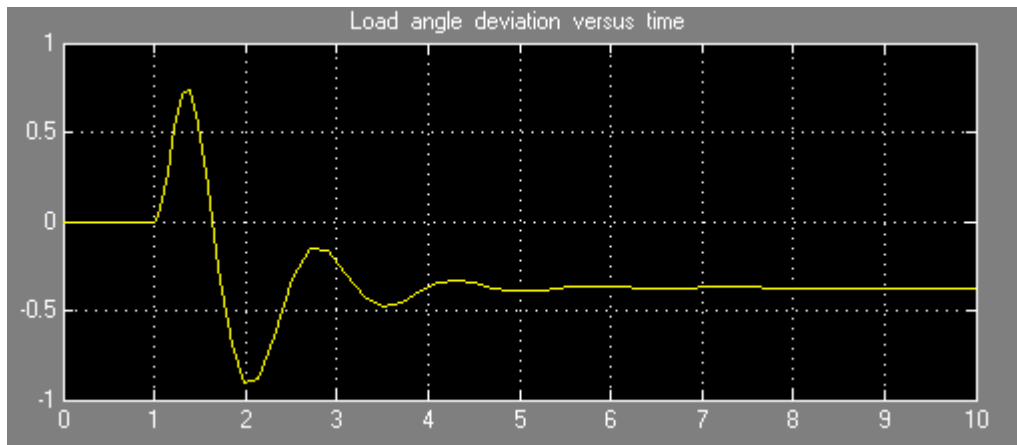


Fig (d)

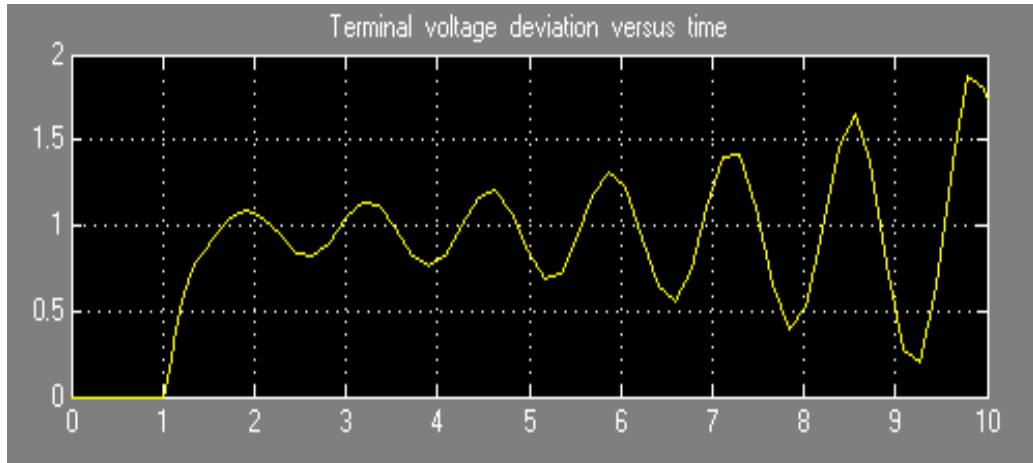


Fig (e)

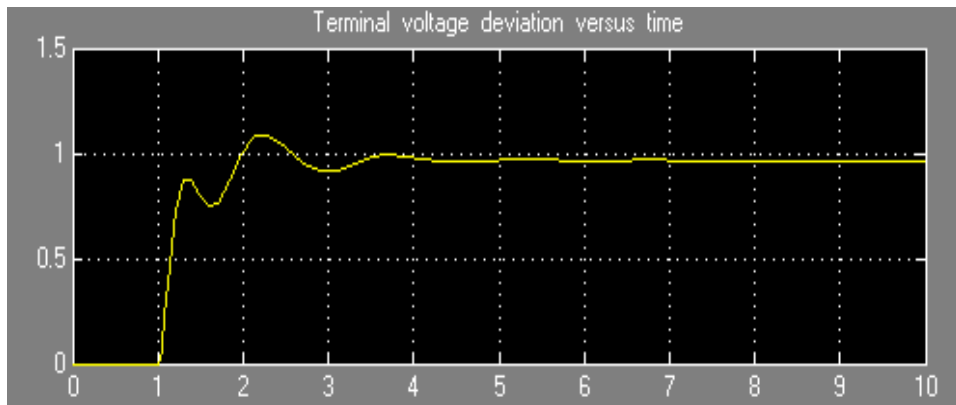


Fig (f)

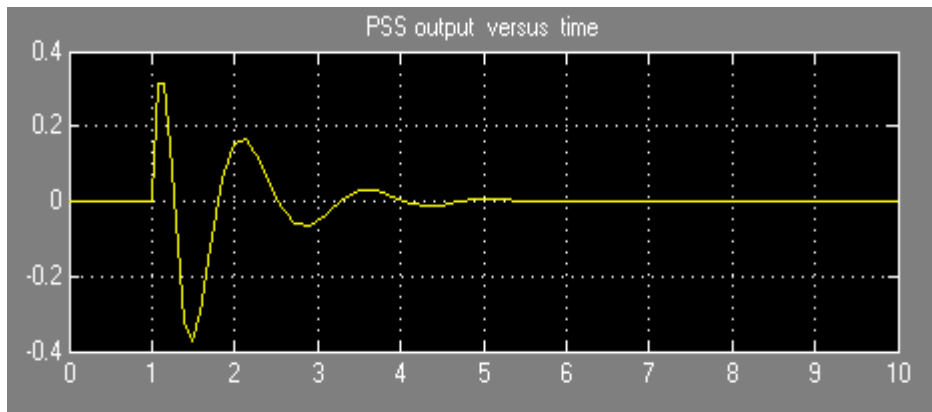


Fig (g)

Fig. 2.12 Response of speed deviation without PSS (a) with CPSS (b) Load angle deviation without PSS (c) with CPSS (d) Terminal voltage deviation without PSS (e) with CPSS (f) PSS output (g)

2.12 Torque characteristics

In the figure shown below the torque characteristics is shown in terms of synchronizing and damping torques for the three cases eg constant excitation, AVR, AVR+PSS. It can be shown from the damping that PSS adds a component of damping which makes the net damping positive.

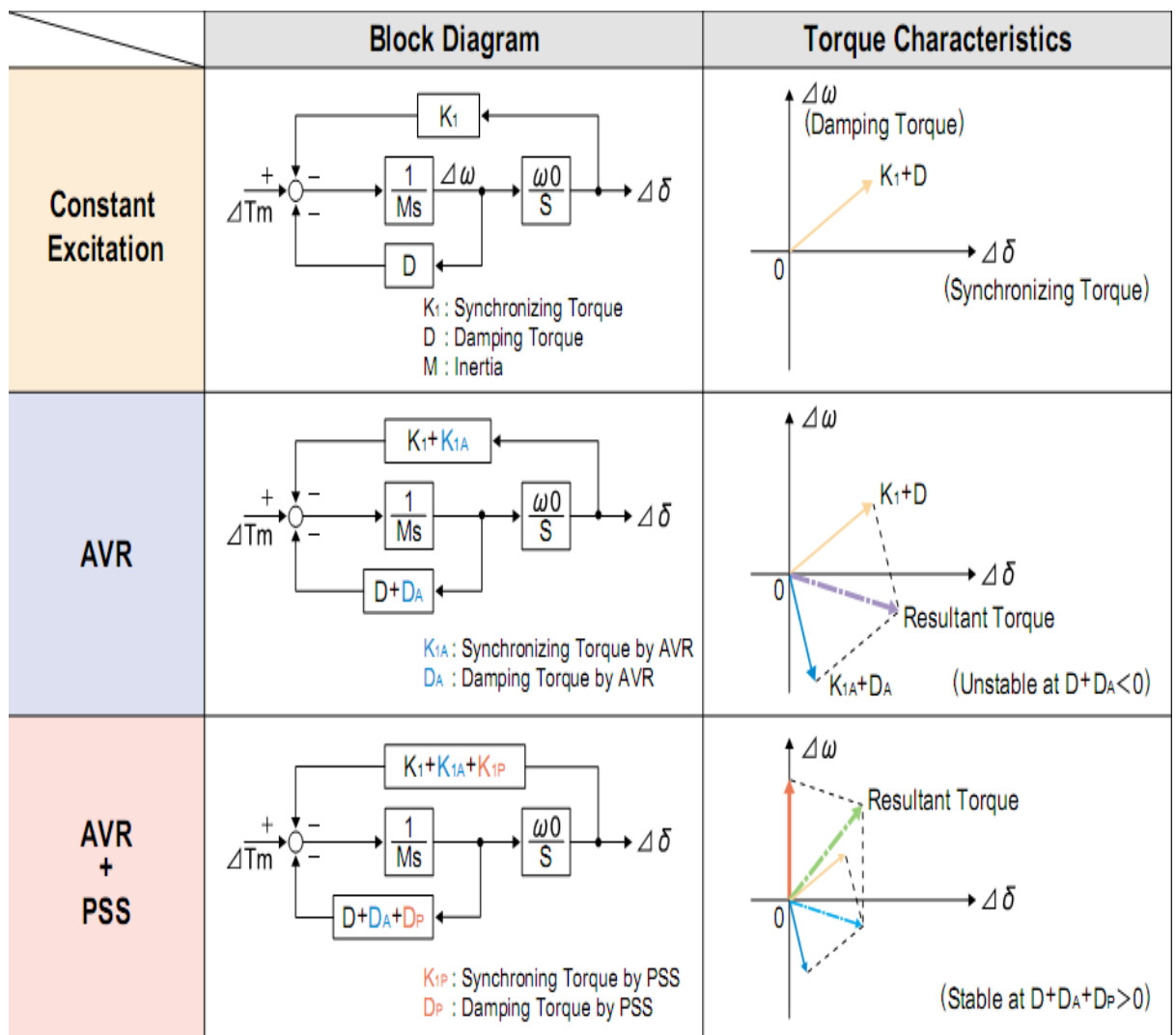


Fig. 2.13 Torque characteristics

It can be shown from the simulation study that after installing the PSS, the system response is well damped. It can be shown from the time responses of linearized model of SMIB system that CPSS is better for particular operating conditions. It may not

yield satisfactory results when there is change in the operating point. The parameters of PSS must be retuned so that it can provide the desired performance . A new method has been proposed for tuning the parameters of a fixed gain power system stabilizer. The stabilizer places the troublesome system modes in an acceptable region in the complex plane and guarantees a robust performance over a wide range of operating conditions. Conventional lead/lag structure is retained but its parameters are retuned using Particle swarm optimization algorithm to obtain enhanced performance.

CHAPTER#3

PARTICLE SWARM OPTIMIZATION

3.1 Introduction

Through cooperation and competition among the population, population-based optimization approaches often can find very good solutions efficiently and effectively. Most of the population based search approaches are motivated by evolution as seen in nature. Four well known examples are genetic algorithms, evolutionary programming, evolutionary strategies and genetic programming. Particle swarm optimization, on the other hand, is motivated from the simulation of social behaviour. Nevertheless, they all work in the same way, that is updating the population of individuals by applying some kinds of operators according to fitness information obtained from the environment so that individuals of the population can be expected to move towards better solution areas.

The PSO algorithm was first introduced by Dr. Russel C. Eberhart and Dr. James Kennedy (1995), inspired by social behavior of bird flocking or fish schooling. The system is initialized with a population of random solutions and searches for optima by updating generations. However, unlike GA, PSO has no evolution operators such as crossover and mutation. In PSO, the potential solutions, called particles, fly through the problem space by following the current optimum particles. Each particle keeps track of its coordinates in the problem space which are associated with the best solution (fitness) it has achieved so far. (The fitness value is also stored.) This value is called *pbest*. Another "best" value that is tracked by the particle swarm optimizer is the best value, obtained so far by any particle in the neighbors of the particle. This location is called *lbest*. when a particle takes all the population as its topological neighbors, the best value is a global best and is called *gbest*.

The particle swarm optimization concept consists of, at each time step, changing the velocity of (accelerating) each particle toward its *pbest* and *lbest* locations (local version of PSO). Acceleration is weighted by a random term, with separate random numbers being generated for acceleration toward *pbest* and *lbest* locations.

In past several years, PSO has been successfully applied in many research and application areas. It is demonstrated that PSO gets better results in a faster, cheaper way compared with other methods.

Another reason that PSO is attractive is that there are few parameters to adjust. One version, with slight variations, works well in a wide variety of applications. Particle swarm optimization has been used for approaches that can be used across a wide range of applications, as well as for specific applications focused on a specific requirement.[6]

3.2 Basic particle swarm optimization

Particle swarm optimization method is based on the social behavior that a population of individuals adapts to its environment by returning to promising regions that were previously discovered. This adaptation to environment is a stochastic process that depends on both the memory of each individual, called particle, and the knowledge gained by the population, called swarm.

In a PSO system, particles change their positions by flying around in a multidimensional search space until a relatively unchanged position has been encountered, or until computational limitations are exceeded. In social science context, a PSO system combines a social-only model and a cognition-only model. The social-only component suggests that individuals ignore their own experience and adjust their behavior according to the successful beliefs of individuals in the neighborhood. On the other hand, the cognition-only component treats individuals as isolated beings. A particle changes its position using these models.

In the numerical implementation of this simplified social model, each particle has three attributes: the position vector in the search space, the current direction vector, the best position in its track and the best position of the swarm. The process can be outlined as follows.

Step1: Generate the initial swarm involving N particles at random.

Step2: Calculate the new direction vector for each particle based on its attributes.

Step3: Calculate the new search position of each particle from the current search position and its new direction vector.

Step4: If termination condition is satisfied, stop. Otherwise, go to step 2.

As the particle can fly in D- dimension search space, the position and velocity of i-th particle can be represented as-

$$X_i = [x_{i1}, x_{i2}, x_{i3}, x_{i4}, \dots \dots x_{iD}],$$

$$V_i = [v_{i1}, v_{i2}, v_{i3}, v_{i4}, \dots \dots v_{iD}],$$

With increased iteration, the swarm will move towards its global best position by keeping track of their personal best. In D- dimensional search space the pbest of i-th particle can be represented as-

$$pbest = [p_{i1}, p_{i2}, p_{i3}, p_{i4}, \dots \dots p_{iD}],$$

and gbest of the whole swarm is presented as-

$$gbest = [g_1, g_2, g_3, g_4 \dots \dots g_D]$$

the new direction vector of the i-th particle at time t, V_i^{t+1} is calculated by the following scheme introduced by Shi and Eberhart.

$$V_{id}^{t+1} = w^t V_{id}^t + c1 R_1^t (pbest_{id}^t - X_{id}^t) + c2 R_2^t (gbest_d^t - x_{id}^t) \quad (3.1)$$

R_1^t and R_2^t are random numbers between 0 and 1. V_{id}^t and X_{id}^t is the velocity and position of the i-th particle in d-th dimension at its time track t. $pbest_{id}^t$ is the best position of the i-th particle (personal best) in d-th dimension in its track at time t and $gbest_d^t$ is the best position of the swarm in d-th dimension at time t. There are three parameters such as the inertia of the particle w^t , and two parameters c1 and c2. Where c1 and c2 are the learning factors which determines the relative influence of the cognitive and social components to update the position and velocity component. Then, new position of the i-th particle at time t, X_{id}^{t+1} , is calculated from-

$$X_{id}^{t+1} = X_{id}^t + V_{id}^{t+1} \quad (3.2)$$

Where X_{id}^t is the current position of the i-th particle at time t. After the i-th particle calculates the next search direction vector V_{id}^{t+1} in consideration of the current search direction vector V_{id}^t , the direction vector going from the current search position X_{id}^t to the best search position in its track $pbest_{id}^t$ and the direction vector going from the current search position X_{id}^t to the best search position of the swarm $gbest_d^t$, it moves from the current position X_{id}^t to the next search position X_{id}^{t+1} calculated by 3.2. In general the parameter w^t is set to large values in the early stage for global search, while it is set to a small values in the last stage for local search.

The inertia weight is used to control the impact of the previous velocities on the current velocity, influencing the trade-off between the global and local experience. Although Zheng claimed that PSO with increasing inertia weight performs better, linear decreasing of the inertia weight is recommended by Shi and Eberhart.[23]

$$w = w_{max} - \left(\frac{w_{max} - w_{min}}{iter_{max}} \right) * iter \quad (3.3)$$

Where w_{max} and w_{min} are maximum and minimum of inertia weight value respectively, $iter_{max}$ is maximum iteration number and $iter$ is the current iteration. A so-called constriction factor K , is factor that increases the algorithm's ability to converge to a good solution and can generate higher quality solution than the conventional PSO approach. In this case, the expression used to update the particle's velocity becomes.

$$V_{id}^{t+1} = K * [w^t V_{id}^t + c1R_1^t (pbest_{id}^t - X_{id}^t) + c2R_2^t (gbest_d^t - X_{id}^t)] \quad (3.4)$$

Where

$$K = \frac{2}{12 - \varphi - \sqrt{(\varphi^2 - 4\varphi)}}, \quad \varphi = c1 + c2, \quad \varphi > 4 \quad (3.5)$$

$$K = 1, \quad \varphi < 4$$

3.3 Flow chart of basic PSO

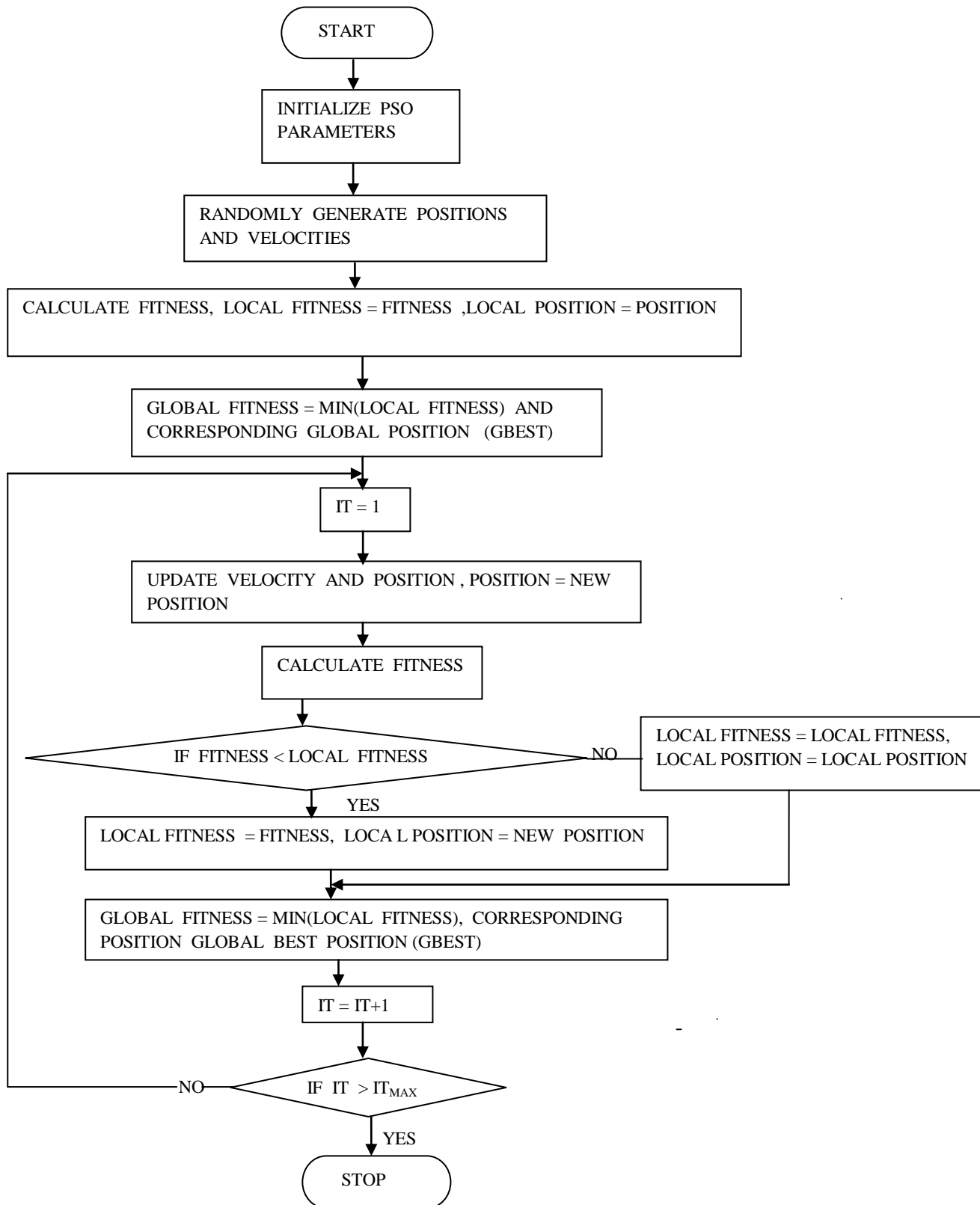


Fig. 3.1 The basic algorithm of PSO

The general search procedure of PSO is shown in figure.

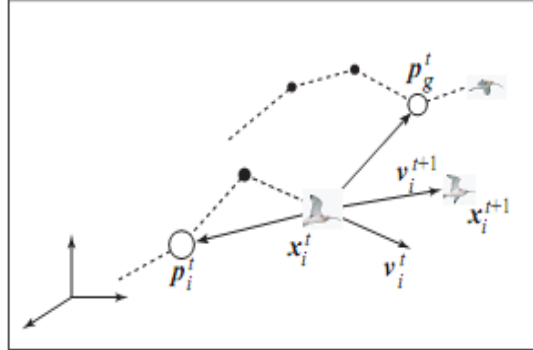


Fig. 3.2 Movement of an individual

Where

x_i^t = current search position of i-th particle at time t.

x_i^{t+1} = next search position of i-th particle.

p_i^t = best search position of i-th particle at time t.

p_g^t = best position of the swarm (global best) at time t.

v_i^t = velocity of i-th particle at time t.

v_i^{t+1} = updated velocity of i-th particle.

If the next search position of the i-th particle at time t, x_i^{t+1} , is better than the best search position in its track at time t, p_i^t , i.e., $f(x_i^{t+1}) \leq f(p_i^t)$, the best search position in its track is updated as $p_i^{t+1} = x_i^{t+1}$. Otherwise, it is updated as $p_i^{t+1} = p_i^t$. Similarly, if p_i^{t+1} is better than the best position of the swarm, p_g^t , i.e., $f(p_i^{t+1}) \leq f(p_g^t)$, then the best position of the swarm is updated as $p_g^{t+1} = p_i^{t+1}$, otherwise it is updated as $p_g^{t+1} = p_g^t$.

3.4 Test example

The effectiveness of PSO is demonstrated through optimizing (minimizing) a test function expressed as

Considering a test function, which has to be minimized-

$$F(x) = \sum_{i=1}^3 (x_i - 50)^6,$$

Number of dimensions = 3,

Number of particles = 100,

C1 = 2, C2 = 2,

Inertia weight = 0.9 to 0.4,

Iterations = 200,

With the developed Matlab programme for the optimization of given function while choosing the above parameters we get the following results.

The global best particle position is (at final iteration)-

x(1,1) x(1,2) x(1,3)

50.0000 50.0000 50.0000

The global best solution (global fitness) is (at final iteration) –

0.0000

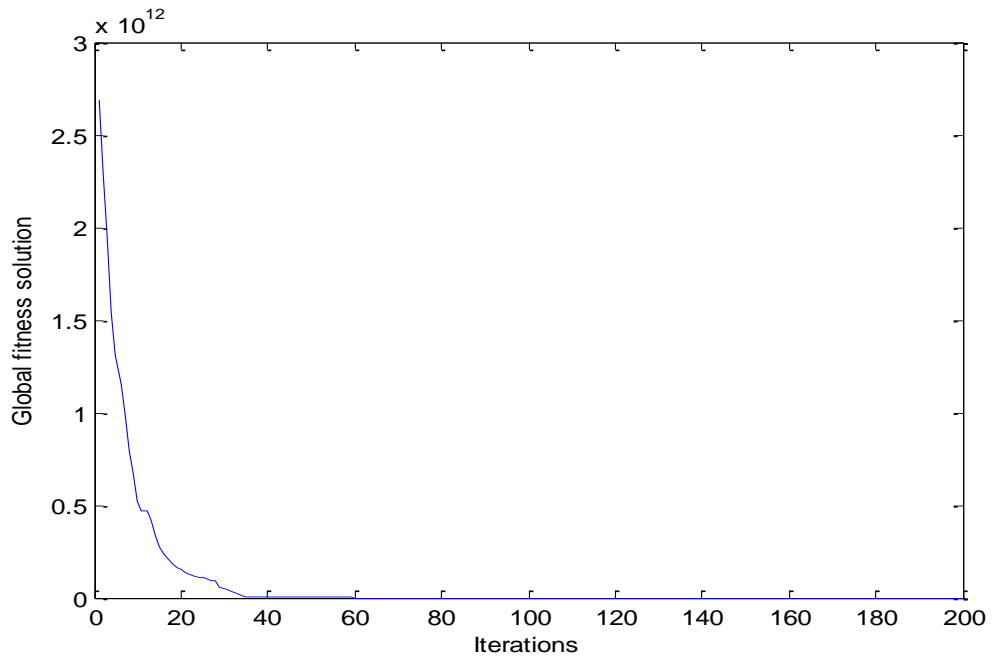


Fig 3.3 The plot of global best solution (fitness) with iterations

It is cleared from the plot that global best solution(fitness) is decreasing with iterations. At final iteration value the global solution is at its optimum value. The plot of global best position of each dimension with iterations is plotted here and shown-

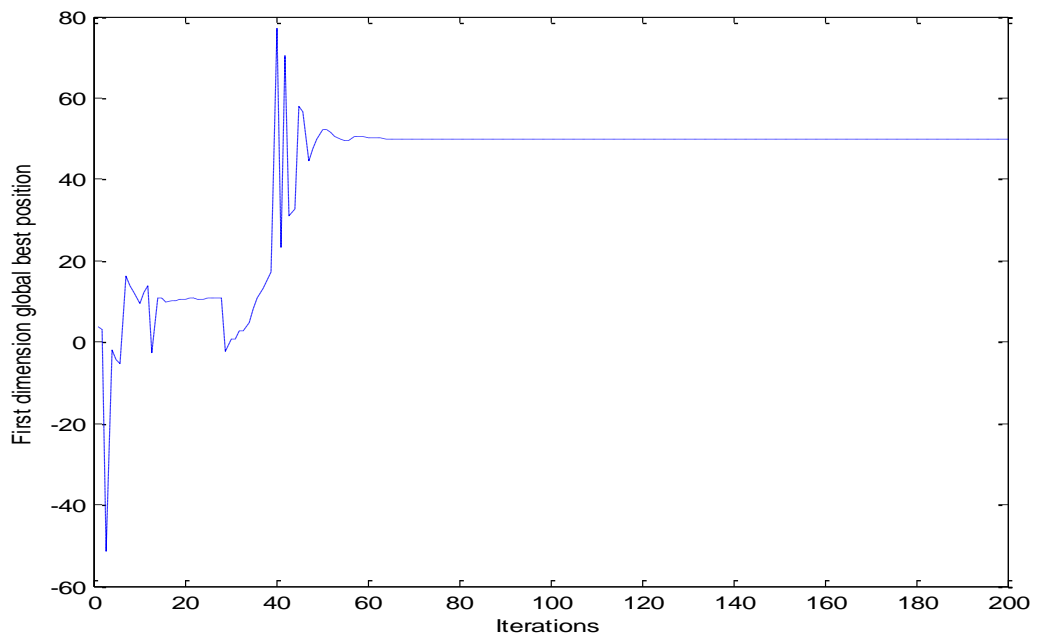


Fig. 3.4 The plot of first dimension global best position with iterations

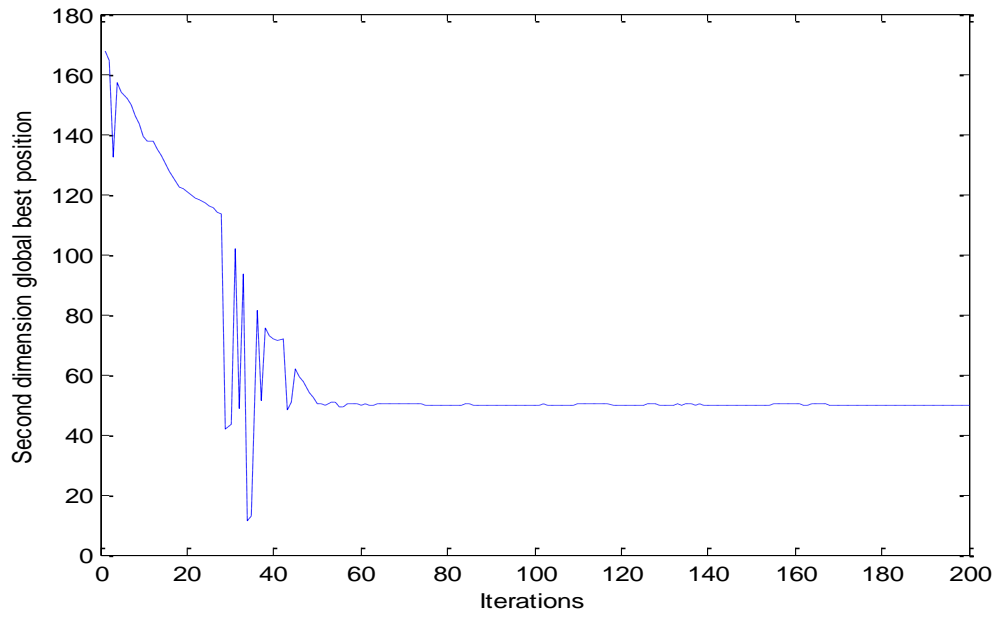


Fig. 3.5 The plot of second dimension global best position with iterations

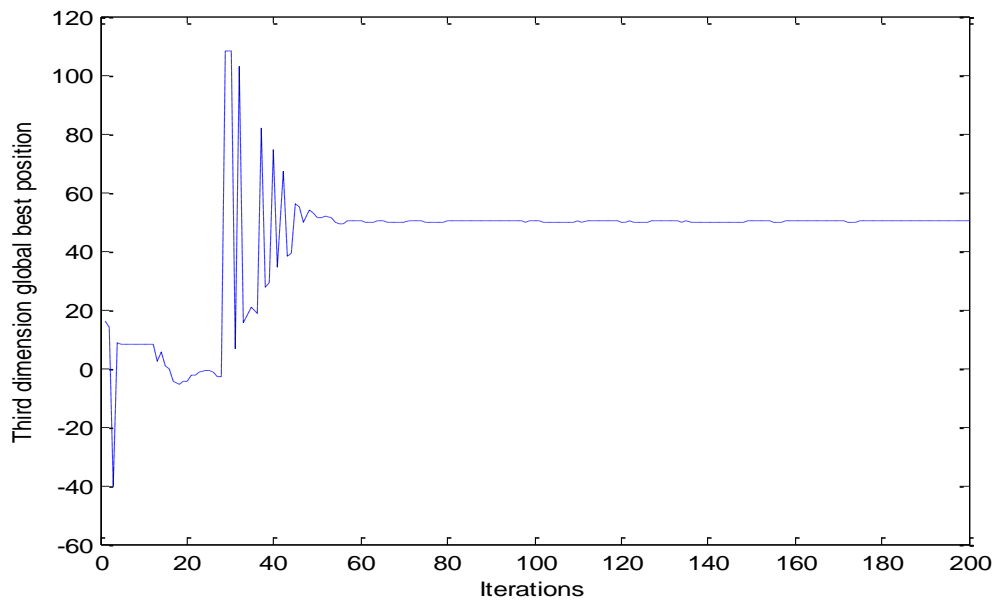


Fig. 3.6 The plot of third dimension global best position with iterations

It is found that there is variation at the start and after that all the dimensions find their optimal value corresponding to optimal fitness of the function.

3.5 Advantages

The advantages of PSO over other traditional optimization techniques can be summarized as follows.

- 1) PSO is a population-based search algorithm (i.e., PSO has implicit parallelism). This property ensures PSO to be less susceptible to getting trapped on local minima.
- 2) PSO uses payoff (performance index or objective function) information to guide the search in the problem space. Therefore, PSO can easily deal with nondifferentiable objective functions. Additionally, this property relieves PSO of assumptions and approximations, which are often required by traditional optimization methods.
- 3) PSO uses probabilistic transition rules and not deterministic rules. Hence, PSO is a kind of stochastic optimization algorithm that can search a complicated and uncertain area. This makes PSO more flexible and robust than conventional methods.
- 4) Unlike GA and other heuristic algorithms, PSO has the flexibility to control the balance between the global and local exploration of the search space. This unique feature of PSO overcomes the premature convergence problem and enhances the search capability.
- 5) Unlike the traditional methods, the solution quality of the proposed approach does not rely on the initial population. Starting anywhere in the search space, the algorithm ensures the convergence to the optimal solution.

CHAPTER#4

PROPOSED STABILIZATION TECHNIQUE

SINGLE MACHINE SYSTEM

4.1 Introduction

Power systems experience low frequency oscillations due to disturbances. These low frequency oscillations are related to small signal stability of power system. The phenomenon of stability of synchronous machine under small disturbances is explored by examining the case of single machine connected to infinite bus. The analysis of SMIB gives physical insight into the problem of low frequency oscillations. These low frequency oscillations are classified into local mode of oscillations, inter area mode of oscillations and torsional mode of oscillations. The single machine connected to infinite bus system is predominant in local mode low frequency oscillations.

These oscillations may sustain and grow to cause system separation if no adequate damping is available. In recent years modern control theory have been applied to power system stabilizer design problems. These include adaptive control, optimal control, variable structure control, and intelligent control.

Despite the potential of modern control techniques with different structures power system utilities still prefer conventional lead/lag power system stabilizer structure. The reason behind that might be the ease of online tuning and lack of assurance of stability related to some adaptive or variable structure techniques.

Recently, global optimization techniques like genetic algorithms (GA), evolutionary programming, Tabu search, simulated annealing and rule based bacteria foraging have been applied for PSS parameter optimization. These evolutionary algorithms are heuristic population based search procedures that incorporate random variation and selection operators. Although, these methods seem to be good methods for the solution of PSS parameter optimization problem. However, when the system has a highly epistatic objective function (i.e. where parameters being optimized are highly correlated), and number of parameters to be optimized is large, then they have degraded efficiency to obtain global optimum solution. A PSO based PSS improves this efficiency.

Here we have considered a case of single machine infinite bus system. A method of particle swarm optimization has been applied for tuning the PSS parameters. A range of operating condition has been considered, over which PSS parameters are obtained through PSO technique.

4.2 Objective function

According to appendix B the equation of D contour is given by-

$$F(z) = \text{Re}(z) - \min[-\zeta |\text{Im}(z)|, a] = 0 \quad (4.1)$$

Where $z \in A$, is a point on the D contour, and A represents the complex plane.

Defining J as

$$J = \max[\text{Re}(\lambda_i) - \min(-\zeta |\text{Im}\lambda_i|, a)] \quad (4.2)$$

$$i = 1, 2, 3, \dots, n$$

Where n is the number of eigen values. λ_i is the i-th eigen value of the system at an operating point. A negative value of J implies that all the eigen values lie on the left of the D contour. If J is positive that implies eigen value is lying on the right of contour.

On these facts objective function F can be defined as

$$F = \begin{cases} J & \text{if } J \leq 0 \\ \alpha * J & \text{if } J > 0 \end{cases} \quad (4.3)$$

Where α is a large positive constant.

The optimization problem can now be stated as:

Minimize F

Subject to:

$$\begin{aligned} K_c^{min} &\leq K_c \leq K_c^{max} \\ T_1^{min} &\leq T_1 \leq T_1^{max} \\ T_2^{min} &\leq T_2 \leq T_2^{max} \end{aligned} \quad (4.4)$$

Where K_c , T_1 , T_2 are the parameters of PSS.

4.3 Algorithm

Step 1. Initialize the set of particles with position value (population), its upper limit and lower limit, random velocities, inertia weight, acceleration constants etc.

Step 2. Calculate the eigen values for each particle from the system modelling.

Step 3. Calculate the objective function for all the eigen values.

Step 4. Set all position values as local best values and fitness values of objective function as local fitness. Find global fitness and its corresponding position value

Step 5. Set $iter = 1$ and compute inertia weight by $w = w_{max} - \left(\frac{w_{max} - w_{min}}{iter_{max}} \right) * iter$

update velocity using velocity update equation for all particles by-

$$V_{id}^{t+1} = w^t V_{id}^t + c1R_1^t (lbest_{id}^t - X_{id}^t) + c2R_2^t (gbest_d^t - x_{id}^t)$$

also check its upper and lower limits.

Step 6. Update position value of particles by

$$X_{id}^{t+1} = X_{id}^t + V_{id}^{t+1}$$

Also check its upper and lower limits.

Step 7. Calculate eigen values for each particle and corresponding fitness values of objective function.

Step 8. Now compare these fitness values to the previous fitness values. Minimum fitness values will be selected as local fitness values and its corresponding position values as local best values. Find minimum of all fitnesses, e.g global fitness value and its corresponding position value.

Step 9. If number of iteration reaches $iter$ go to step 10, otherwise go to step 5.

Step 10. Particle with minimum fitness value is the optimum particle.

4.4 Flow chart

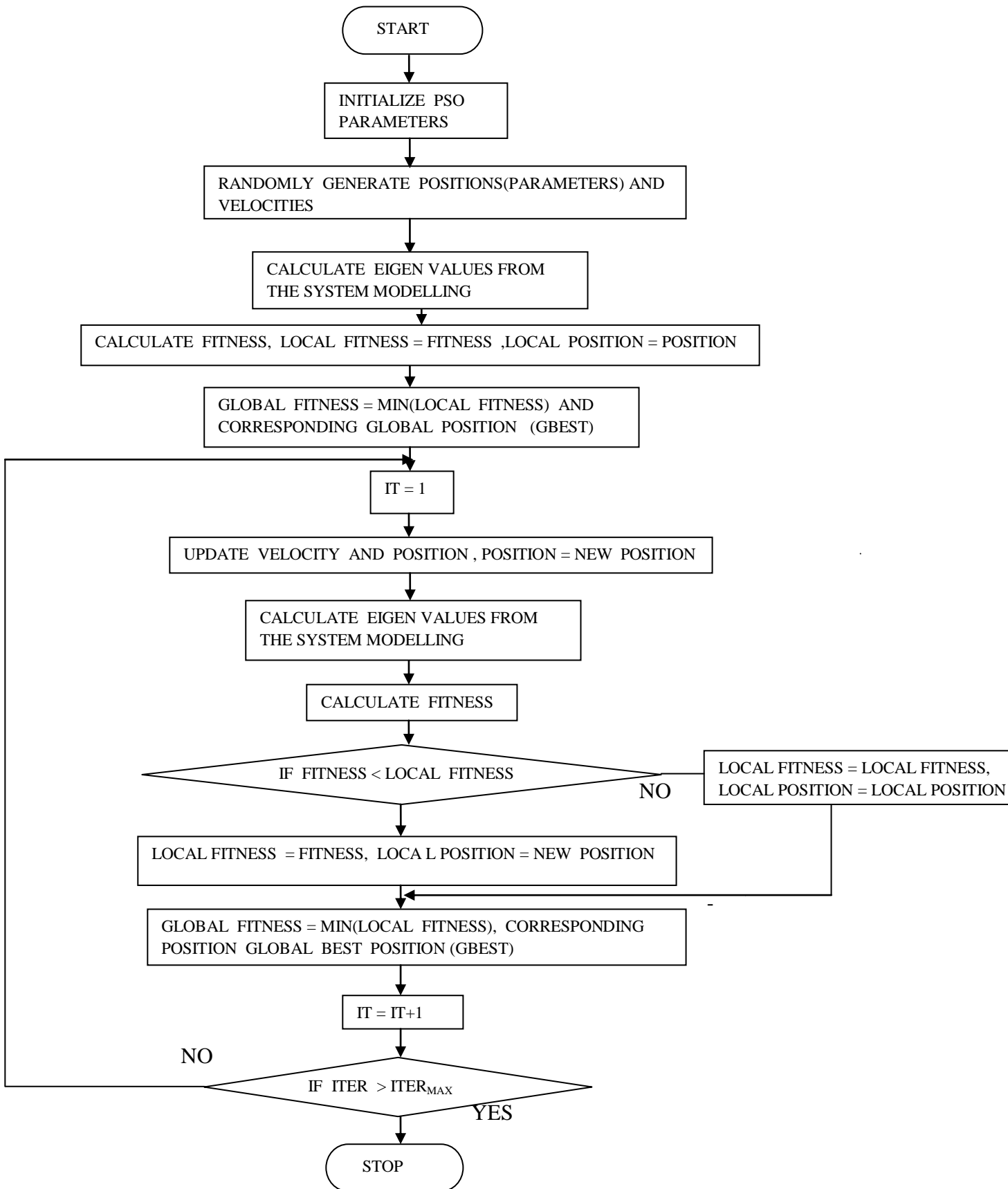


Fig. 4.1 The basic algorithm of PSO in optimization approach

CHAPTER#5

RESULTS, CONCLUSION & FUTURE SCOPE

The PSO is applied to the problem for starting operating condition of $P = 0.9$, $Q = 0.1$, $X_e = 0.997$. The desired setting of damping ratio ' ζ ' and reference line value 'a' in equation 4.2 has been selected as 0.2 and -1.5 respectively. The search area for the PSS Parameters is as follows-

Kc	T ₁	T ₂
1 - 50	0.1 – 0.6	0.1 – 0.6

Table 5.1 Bounds on Stabilizer Parameters

No of particles (parameters)	C ₁	C ₂	W (inertia weight)
100	2	2	0.9 – 0.4

Table 5.2 PSO Parameters

PSS parameters are initialized randomly in the algorithm. PSO algorithm is run for the set number of iterations to find the optimum parameters. Some undamped and lightly damped modes are shifted towards the left of the contour ensuring the robustness in the design. The second column of the table 5.3 shows the modes that are shifted towards the contour.

Randomly initialized Eigenvalues ($P = 0.9$, $Q = 0.1$, $X_e = 0.997$)	After applying PSO algorithm
-2.2157 , -15.3219 , -0.2307 + 6.7845i -0.2307 - 6.7845i, -4.5688, -0.1019 -2.0754	-10 , -18.4261, -1.5001 + 6.2374i -1.5001 - 6.2374i, -0.1011 -4.3932 + 4.5679i, -4.3932 - 4.5679i
-1.8650 , -10.6290 + 2.4148i, -10.6290 - 2.4148i, 0.5149 + 5.0835i 0.5149 - 5.0835i, -0.1001 , -1.8504	-10, -18.4260, -1.5000 + 6.2255i -1.5000 - 6.2255i, -0.1011, -4.3933 + 4.5839i, -4.3933 - 4.5839i

-2.0448, -10.6833 + 2.5073i -10.6833 - 2.5073i, 0.5315 + 5.1389i 0.5315 - 5.1389i, -0.1003, -1.9545	-10, -18.4260, -1.5000 + 6.2240i -1.5000 - 6.2240i, -0.1011, -4.3933 + 4.5859i, -4.3933 - 4.5859i
-3.6586, -13.3183, 0.0923 + 5.5522i 0.0923 - 5.5522i, -0.1006, -6.6087 -4.1294	-10, -18.4261, -1.5001 + 6.2205i -1.5001 - 6.2205i, -0.1011 -4.3932 + 4.5908i, -4.3932 - 4.5908i
-3.2416, -15.3104, -0.5604 + 6.2346i -0.5604 - 6.2346i, -0.1008, -3.5117 + 2.0456i, -3.5117 + 2.0456i	-10, -18.4261, -1.5001 + 6.2220i -1.5001 + 6.2220i, -0.1011, -4.3932 + 4.5888i, -4.3932 - 4.5888i

Table 5.3 Random eigenvalues col 1, shifted eigenvalues col 2

T₁	T₂	K_c
0.2430	0.10	24.2646

Table 5.4 Optimum parameters in the final run of the algorithm

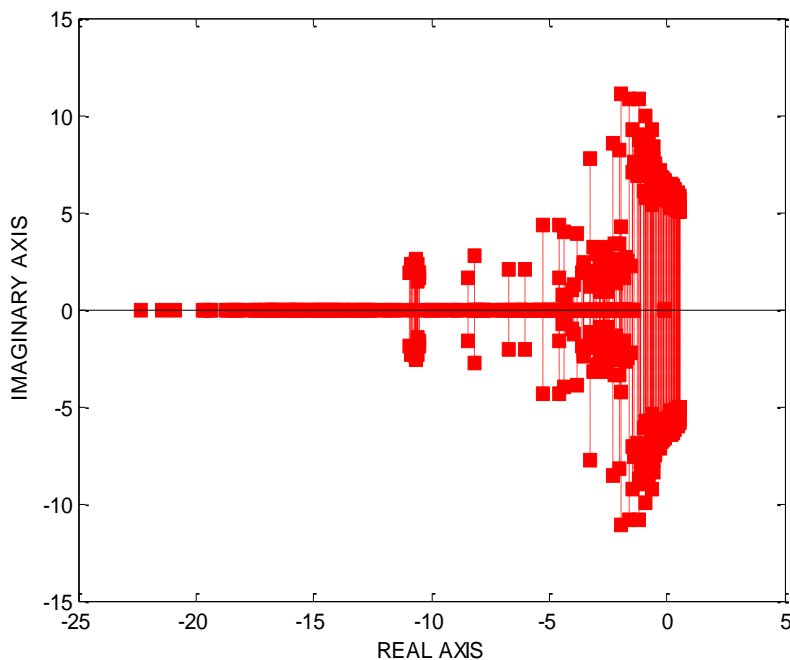


Fig 5.1 Randomly initialized Eigen values in the complex plane

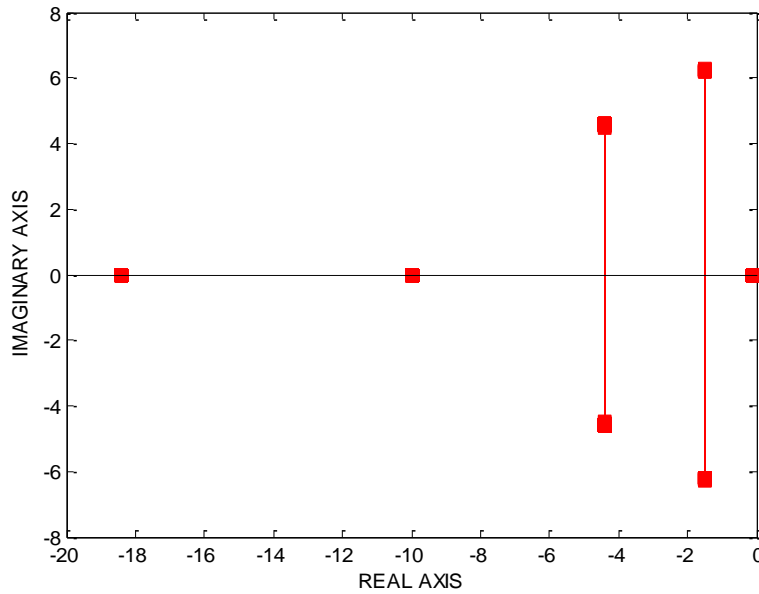


Fig 5.2 Shifted eigenvalues with respect to D- Contour

Due to perturbation, the dynamics of the system changes. So for the perturbed dynamics the PSO can effectively find the optimum parameters too. We have given a perturbation to the dynamics to investigate the effectiveness of PSO. In the table 5.5 below (first column), eigen values are shown for the perturbed dynamics. First column is showing the modes obtained from the best parameters of previous operating point. Second column shows the modes that are shifted towards the contour.

Eigen values with Changed operating condition (P = 0.8, Q = 0.0, Xe = 0.897)	After applying PSO algorithm
-10, -18.3117, -1.1744 + 6.6687i -1.1744 - 6.6687i, -0.1009 , -4.7800 + 4.4046i, -4.7800 - 4.4046i	-10, -18.6720, -1.5002 + 6.6292i -1.5002 - 6.6292i, -0.1009, -4.2741 + 4.7834i , -4.2741 - 4.7834i
-10, -18.3116 , -1.1748 + 6.6601i -1.1748 - 6.6601i, -0.1009 -4.7797 + 4.4171i, -4.7797 - 4.4171i	-10, -18.6707, -1.5002 + 6.6155i -1.5002 - 6.6155i, -0.1009, -4.2748 + 4.8003i, -4.2748 - 4.8003i
-10, -18.3116, -1.1749 + 6.6591i -1.1749 - 6.6591i, -0.1009, -4.7796 + 4.4187i, -4.7796 - 4.4187i	-10, -18.6696, -1.5001 + 6.6050i -1.5001 - 6.6050i , -0.1009, -4.2755 + 4.8131i , -4.2755 - 4.8131i

-10 , -18.3117, -1.1750 + 6.6565i -1.1750 - 6.6565i, -0.1009 -4.7794 + 4.4225i, -4.7794 - 4.4225i	-10, -18.6700 , -1.5005 + 6.6051i -1.5005 - 6.6051i, -0.1009 , -4.2748 + 4.8133i, -4.2748 - 4.8133i
-10, -18.3117, -1.1750 + 6.6576i -1.1750 - 6.6576i, -0.1009 , -4.7795 + 4.4209i, -4.7795 - 4.4209i	-10, -18.6706, -1.5000 + 6.6163i -1.5000 - 6.6163i, -0.1009, -4.2750 + 4.7990i, -4.2750 - 4.7990i

Table 5.5 Eigen values for the perturbed dynamics col1, Shifted eigenvalues col2

T_1	T_2	K_c
0.2810	0.1000	22.6741

Table 5.6 Optimum parameters in the final run of the algorithm

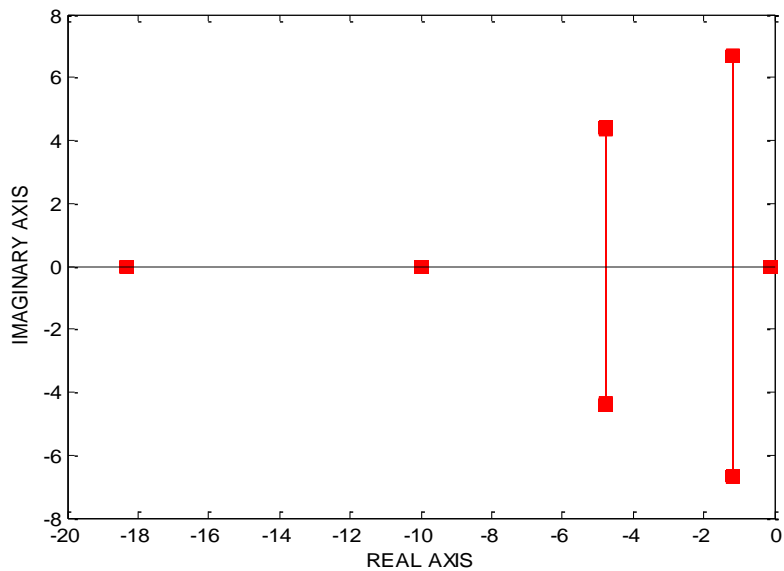


Fig 5.3 Eigen values corresponding to the local best parameters of the previous operating point

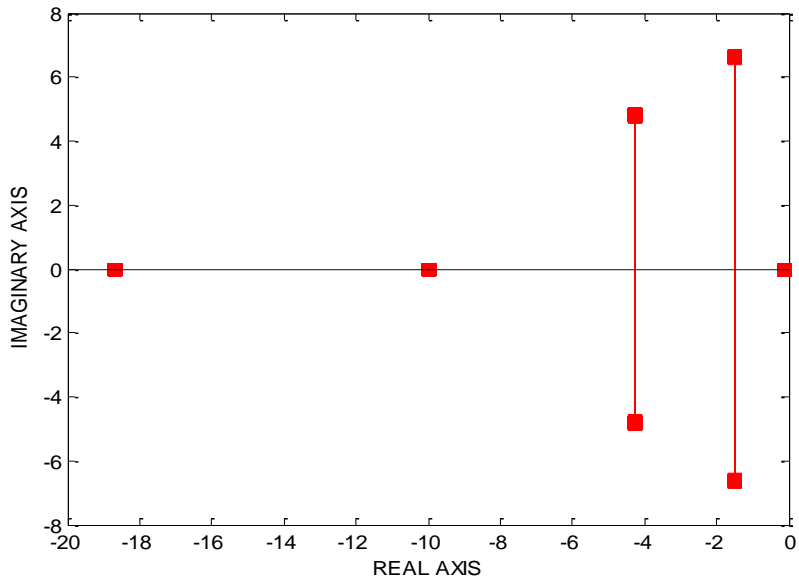


Fig 5.4 Shifted eigenvalues with respect to D- Contour

5.1 Time domain simulation

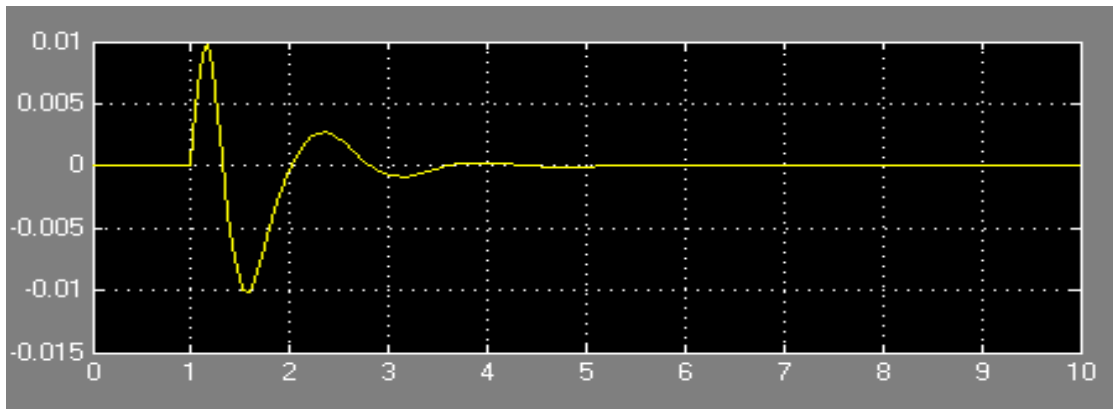


Fig (a)

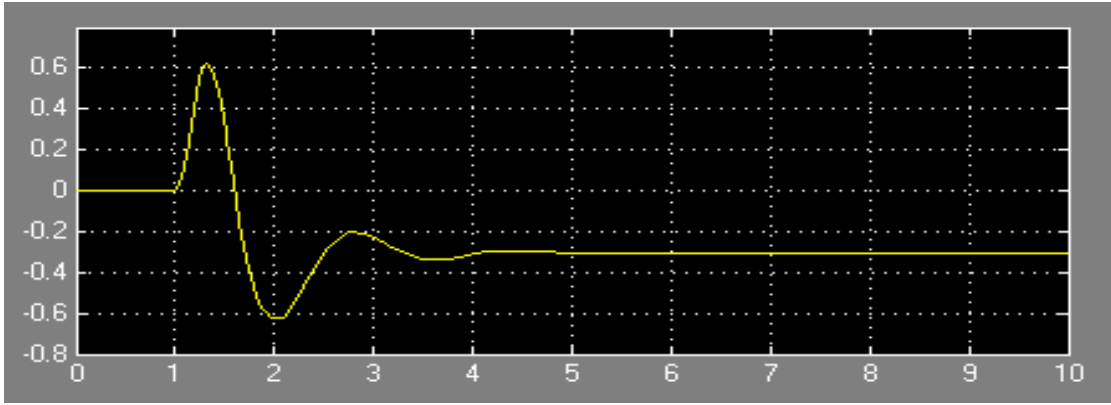


Fig (b)

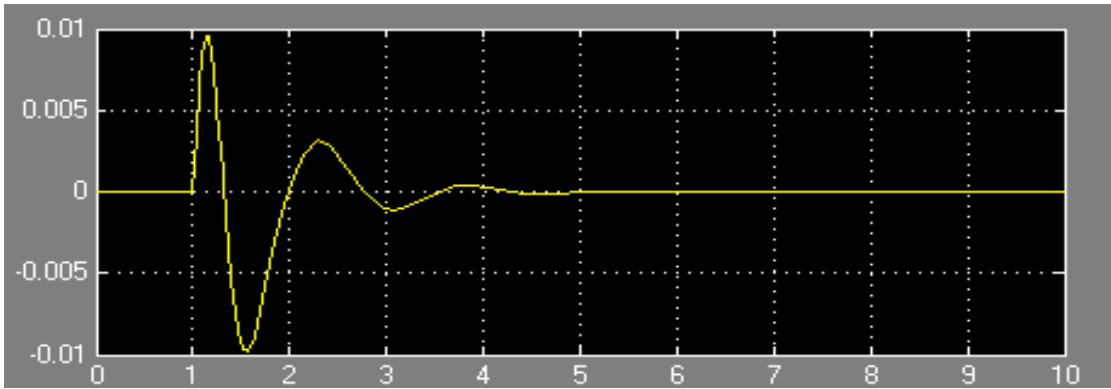


Fig (c)

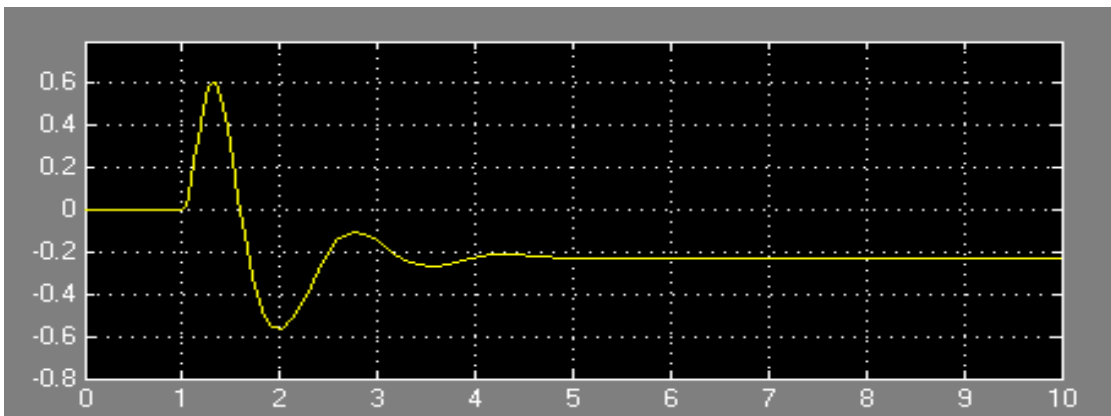


Fig (d)

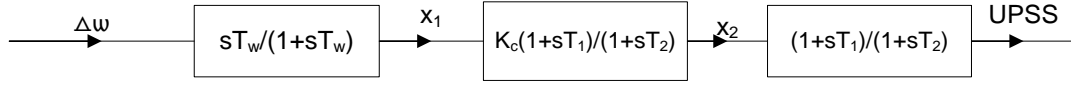
Fig 5.5 Response of speed deviation and Load angle deviation ($P = 0.9, Q = 0.1, X_e = 0.997$) (a), (b) ($P = 0.8, Q = 0.0, X_e = 0.897$) (c), (d)

5.2 Conclusion & Future scope

An optimal design of power system stabilizer in single machine system using PSO technique has been proposed. The technique shifts the lightly damped or undamped modes to prescribed zone in the complex plane. The design problem of PSS parameters is converted into an optimization problem which is solved by PSO technique. Eigen value analysis give the satisfactory damping on system modes, especially the low frequency modes. Time domain simulations show that oscillations of synchronous machine can be quickly and effectively damped for power systems with the proposed with proposed PSS over a range of operating condition.

The discussed formulation can be extended to the multimachine power systems ensuring optimization of multiple PSS parameters.

APPENDIX A



From the above block diagram the state equations can be written as-

$$s x_1 = \Delta w s - \frac{x_1}{T_w}$$

$$s x_1 = -\frac{K_1}{M} \Delta \delta - \frac{D}{M} \Delta w - \frac{K_2}{M} \Delta E'_q - \frac{x_1}{T_w} \quad (\text{A. 1})$$

Similarly-

$$s x_2 = -\frac{K_c K_1 T_1}{T_2 M} \Delta \delta - \frac{D}{M} K_c \frac{T_1}{T_2} \Delta w - \frac{K_c K_2 T_1}{T_2 M} \Delta E'_q + \left(\frac{K_c}{T_2} - \frac{K_c T_1}{T_2 T_w} \right) x_1 - \frac{x_2}{T_2} \quad (\text{A. 2})$$

$$s UPSS = \frac{K_c K_1}{M} \left(\frac{T_1}{T_2} \right)^2 \Delta \delta - \frac{D}{M} K_c \left(\frac{T_1}{T_2} \right)^2 \Delta w - \frac{K_c K_2}{M} \left(\frac{T_1}{T_2} \right)^2 \Delta E'_q + \left(\frac{K_c T_1}{T_2^2} - \frac{K_c T_1^2}{T_2^2 T_w} \right) x_1 + \left(\frac{1}{T_2} - \frac{T_1}{T_2^2} \right) x_2 - \frac{UPSS}{T_2} \quad (\text{A. 3})$$

From the help of above state equations the eigen values of the system can be obtained.

K_c , T_1 , T_2 are the PSS parameters. The K constants of the machine for SMIB system can be calculated from the following equations.

$$K_1 = \frac{E_{q0} V_b}{X_{qT}} \cos \delta_0 + \frac{(X_q - X'_d)}{X_{dT'}} i_{q0} V_b \sin \delta_0 \quad (\text{A. 4})$$

$$K_2 = \frac{V_b}{X_{dT'}} \sin \delta_0 \quad (\text{A. 5})$$

$$K_3 = \frac{X_{dT'}}{X_{dT}} \quad (\text{A. 6})$$

$$K_4 = \frac{(X_d - X'_d)}{X_{dT'}} V_b \sin \delta_0, \quad (A.7)$$

$$K_5 = -\frac{X_q V_{d0}}{X_{qT} V_{t0}} V_b \cos \delta_0 - \frac{X'_d V_{q0}}{X_{dT'} V_{t0}} V_b \sin \delta_0 \quad (A.8)$$

$$K_6 = \frac{X_E V_{q0}}{X_{dT'} V_{t0}} \quad (A.9)$$

Where

$$X_{dT'} = X'_d + X_E$$

$$X_{dT} = X_d + X_E$$

$$X_{qT} = X_q + X_E$$

SYSTEM DATA

f (Hz)	D(pu)	X _d (pu)	X' _d (pu)	X _q (pu)	H(sec)	T' _{do} (sec)	X _E (pu)	R _E (pu)
50	0	0.973	0.19	0.55	4.63	7.765	0.997	0

Table A.1

AVR PARAMETERS

K _A	T _A
50	0.05

Table A.2

APPENDIX B

DERIVATION OF EQUATION 4.1

Consider the figure B.1

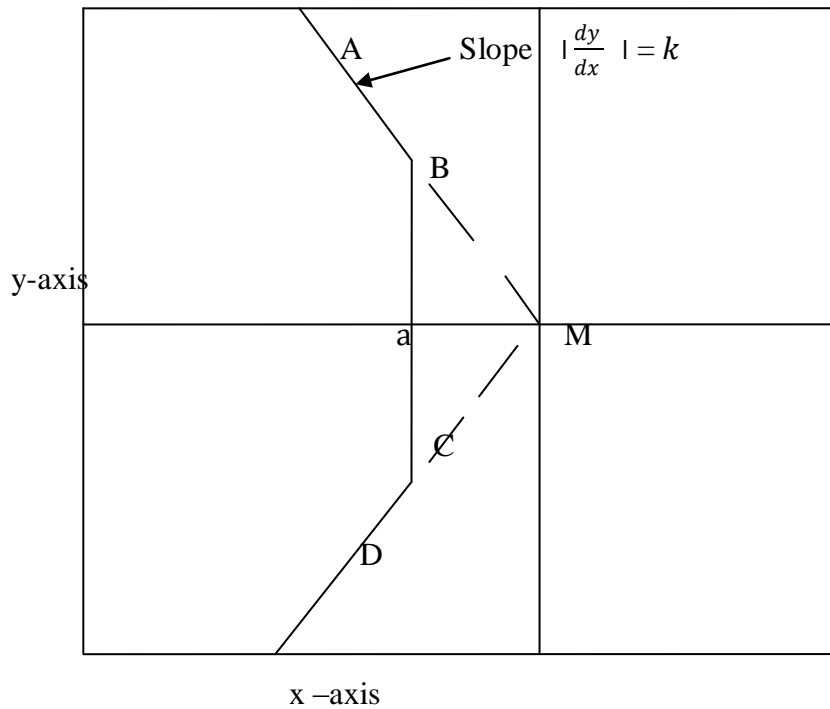


Fig. B.1 D –contour in x – y plane

The equations of line ABM and DCM in x-y plane can be written as:

$$x = -\frac{1}{k} |y| \quad (B.1)$$

$$\frac{1}{k} |y| + x = 0$$

Where k is the modulus of the slope of line. The equation of the line BC can be written a

$$x - a = 0 \quad (B.2)$$

Combining equations B.1 and B.2 the equation of D contour ABCD can be written as-

$$x - \min(-|y|/k, a) = 0 \quad (\text{B.3})$$

If $-1/k = \zeta$, then in reference of complex plane the equation B.3 becomes-

$$\text{Re}(z) - \min(-\zeta |\text{Im}(z)|, a) = 0 \quad (\text{B.4})$$

Where $x = \text{Re}(z)$, and $y = \text{Im}(z)$

$$z = x + iy$$

REFERENCES

- [1] Concordia C, Demello F.P, “Concepts of Synchronous Machine Stability as Effected by Excitation Control”, *IEEE Transactions on Power Apparatus and Systems*, Vol. PAS-88, No 4, pp. 316-329. April 1969.
- [2] Anderson A, Faud A.A, “Power System Control and Stability”, Iowa State University Press, 1977.
- [3] Bacalao N.J, Diaz R, Feijoo B, Flores L, Urdaneta A.J, “Tuning of Power System Stabilizers Using Optimization Techniques”, *IEEE Transactions on Power Systems*, Vol. 6, No. 1, PP 127-134, Feb. 1991.
- [4] Champagne R, Grondin R, Kamwa I, Potvin J, Soulieres L, “PSS Design for Transient Stability Improvement through Supplementary Damping of the Common Low Frequency”, *IEEE Transactions on Power Systems*, Vol. 8, No. 3, , August. 1993.
- [5] Kundur P, “POWER SYSTEM STABILITY AND CONTROL”, McGraw-Hill 1994.
- [6] Eberhart R, Kennedy J, “Particle Swarm Optimization”, PP. 1942 – 1948, *IEEE Conference*, 1995
- [7] Lawson R, Murdoch A, Pearson W. R., Venkataraman S., “Integral of Accelerating Type PSS Part 1 – Theory, Design, and Tuning Methodology”, *IEEE Transactions on Energy Conversion*, Vol. 14, No. 4, PP. 1658 – 1663, December 1999.
- [8] P Kundur, “Effective use of Power Stabilizers for Enhancement of Power System Reliability”, *IEEE Power engineering society Summer meeting*, vol. 1, pp. 96-103, July 1999
- [9] Eberhart R.C, Shi Y, “Empirical Study of Particle Swarm Optimization”, *Proceedings of the 1999 Congress on Evolutionary Computation* ,1999, CEC.99, PP. 1945 – 1950, 1999.

- [10] Abdel - Magid Y.L, Abido M.A, “Robust Design of Multimachine Power System Stabilizers Using Tabu Search Algorithm”, *IEEE Proceedings, Generation, Transmission and Distribution*, Vol. 147, Issue: 6, PP. 387-394, 2000
- [11] Abido M.A, “Robust Design of Power System Stabilizers Using Simulated Annealing”, *IEEE Transactions on Energy Conversion*, Vol. 15, Issue: 3, PP. 297-304, 2000.
- [12] Abdel-Magid Y.L, Abido M, Mantaway A.H, “Robust Tuning of Power System Stabilizers in Multimachine Power Systems”, *IEEE Transactions on Power Systems*, Vol. 15, issue: 2, PP. 735-740, 2000.
- [13] Abdel –Magid Y.L, Abido M, “Optimal Design of Power System Stabilizers Using Evolutionary Programming”, *IEEE Transactions on Energy Conversion*, Vol. 17, Issue: 4, PP. 429-436, 2002.
- [14] Padiyar K.R, “Power System Dynamics, Stability and Control”, Second Edition, Hyderabad, B.S. Publication, 2002.
- [15] Abdel-Magid Y.L, Abido M.A, “Optimal Design of Robust Power System Stabilizers Using Genetic Algorithms”, *IEEE Transactions on Power Systems*, Vol. 18, Issue: 3, PP. 1125-1132, 2003.
- [16] Monavar H, Rashidi F, Rashidi M, “Tuning of Power System Stabilizers via Genetic Algorithm for Stabilization of Power systems”, *IEEE International Conference on Systems, Man & Cybernetics*, Vol. 5, PP. 4649-4654, 2003.
- [17] Ma Long-Hua, Qian Ji-Xin, Zhang Li-yan, Zheng Yong-Ling, “Empirical Study of Particle Swarm Optimizer with Increasing Inertia Weight”, *The 2003 Congress on Evolutionary Computation*, Vol. 1, PP. 221 – 226, 2003.
- [18] Boukarim G E, Chow J.H, Murdoch A, “Power System Stabilizers as a Undergraduate Control Design Projects”, *IEEE Transactions on Power Systems*”, Vol. 19, No. 1, PP. 144-151, Feb 2004.
- [19] Dubey M, Gupta P, “Design of Genetic Algorithm Based Robust Power System Stabilizer”, *International Journal of Computational Intelligence* 2;1, PP. 48 – 52, 2006.

- [20] Moore P.W, Venayagamoorthy G.K., “Empirical Study of an Unconstrained Modified Particle Swarm Optimization”, *IEEE Congress on Evolutionary Computation*, PP. 1477 – 1482, 2006.
- [21] Gurrala G, Sen I, “A Modified Heffron-Phillip’s Model for The Design of Power System Stabilizers”, *Power System Technology and IEEE Power India Conference*, PP. 1-6, 2008.
- [22] Zellagui M, “Robust Power System Stabilizer Design Using Genetic Local Search Technique for Single Machine Connected to Infinite Bus”, *International Journal of Signal System Control & Engineering Application*1(3): PP. 188-194, 2008,ISSN: 1997 – 5422.
- [23] Kato K, Matsumoto K, Matsui T, Sakawa M, Uno T., “Particle Swarm Optimization for Non Linear Integer Programming Problem”, *Proceedings of International MultiConference of Engineers and Computer Scientists*, Vol. II, March 2008, Hongkong.
- [24] Liu J.Y, Long C., Luo Q, Lu L., “An Improved Particle Swarm Optimization Algorithm”, *IEEE Conference on Granular Computing*, PP. 486- 490, 2008.
- [25] Al – Hinai, Al – Hinai SM, “Dynamic Stability Enhancement Using PSO Power System Stabilizer”, *2-nd International Conference on Adaptive Science & Technology*, 2009, ICAST 2009, PP. 117-119.